Dissipative Homogenised Reinforced Concrete (DHRC) constitutive model devoted to reinforced concrete punts

Abstract:

This documentation present the theoretical formulation and numerical integration of the DHRC constitutive law, acronym for “dissipative homogenised reinforced concrete” used with modelling DKTG punts. “Total” It is one of models called used to thin structures (beams, punts and shells). Nonlinear phenomena such ace plasticity gold ramming, are directly related to the generalized strains (extension, curvature, distortion) and generalized stress (membrane forces, bending and cutting edges). So, this constitutive law is applied with has finite element punt gold Shell. Compared to has multi-layered approach, CPU time and memory are saved. The advantage over multi-to bush-hammer shells is even more important when the constituents of the punt behaves in has quasi-brittle manner (concrete, for example), total ace the model avoids localization exits.

The DHRC constitutive law idealize both ramming and irreversible deformation under combined membrane resulting stress and bending of reinforced concrete punts using “homogenised” parameters. Constitutive This law represents year evolution of the GLRC_DM constitutive model which idealize only ramming in membrane and bending situations. Unlike GLRC_DM, the DHRC constitutive model has supplements theoretical justification by using the theory of periodic homogenization: it idealize the effects of steel-concrete slipway in addition to the concrete degradation of stiffness from the diffuses cracking, the bending-membrane coupling in has consist way and accounts for the orthotropy and possible asymmetries coming from steel reinforcement grids. The DHRC macroscopic constitutive law is not softening: this avoids solving problems throughout the structural analysis.

Constitutive The parameter setting of this law results of the particular characteristics of concrete and steel materials used, and the geometrical characteristics of the section, the thickness ratio of steel rebar, positions and directions, which are input dated of has identification representative procedure from the answers of elementary volumes of the section of the reinforced concrete punt. Total The to use parameter number is 21 : 11 geometrical parameters and 10 material parameters.

Contents

1 Introduction

1.1 Total modelling

Concrete Reinforced has heterogeneous material constituted of ribbed gold lime pit steel rebar and concrete. The rebar cuts regular spacing one the two directions x and y in the plane. We consider moderate cycling gold alternate loading conditions: the material is therefore considered ace has continuum.

With total constitutive punt model devoted to structural element generally means that the constitutive law is written directly in terms of the relationship between the generalized stress and generalized strains. Applicable The overall approach of the structures behavior modeling is particularly to composite structures, such ace reinforced concrete (see Figure 1.1-a), and this represents local year alternative to the so-called approaches but semi-total ones, which are finer goal more expensive models (see [bib5] and [bib6]). In the local approach has thin model is used for each phase (steel, concrete) and to their interactions (adhesion). In the semi-total approach one exploits the slenderness of the structure to simplify the description of the kinematics, it leading to “PMF” models (multi-beam fiber) but multi-to bush-hammer shells.

The uses of the theory of punts and thin shells edge effectively describe the mechanical behaviour of reinforced concrete structures, which are usually slender; indeed we uses this constitutive modelling in the context of Coils-Kirchhoff' S kinematics, see [feeding-bottle 16] and [feeding-bottle 17].

Structural The interest of the overall model dregs in the fact that the finite element requires only has single point of integration in the element thickness and also in the uses of has homogenized behaviour. This concrete advantage is even more important in the analysis of reinforced, since it bypasses the concrete localization problem encountered in the modelling of without reinforcement. Obviously, has total model idealize local phenomena of has coarse manner and requires more validation prior to its application to industrial situations. Finally, it is impossible ace soon ace we consider the non-linear phase behaviour back locally to provide field been worth, except strain fields.

This simplified modelling approach edge Be enhanced by year appropriate calibration of the overall parameters.

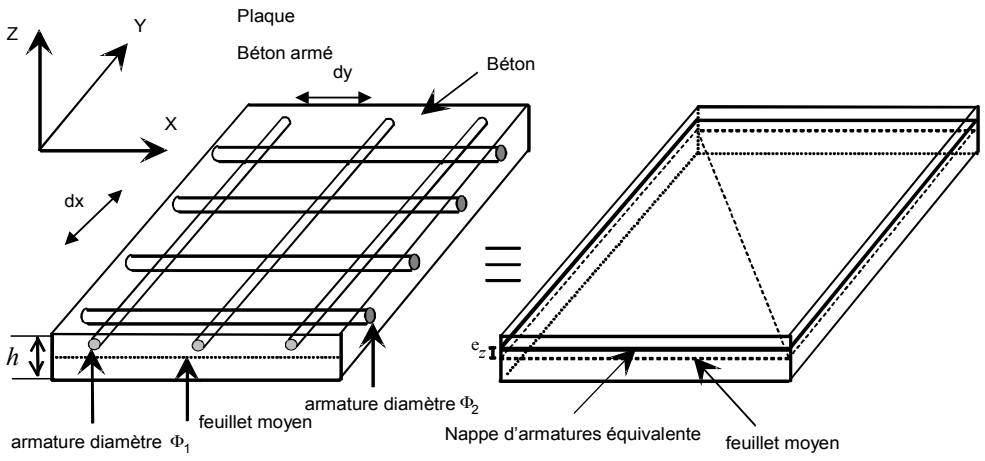

Figure 1.1-a : reinforced concrete slab.

1.2 Objective of the DHRC constitutive model

The DHRC constitutive model, named for “dissipative homogenised reinforced concrete”, is whitebait to idealize the stiffness degradation of has reinforced concrete punt, for has quite moderate load arranges, i.e without reaching the collapse, ace the GLRC_DM constitutive model does, see [R7.01.32], We edge refer to the published papers [bib12, bib13] for extensive explanations; however this *Code_Aster* Reference document reuses the hand shares of [bib13]. Nevertheless, DHRC brings important year enhancement of the GLRC_DM model: (1) it is based one has full theoretical formulation from the local analysis, (2) it involves natively the membrane-bending coupling, (3) accounts for any standard of rebar grids in the thickness (e.g different upper and lower grids, but rebar with distinct sections one the two Ox and Oy directions), In that judicious, DHRC constitutive model IS more representative than GLRC_DM.

The reference frame is constituted by the two directions x and y of steel rebar in the plane. The to use local edge define thesis two directions with the command, see [U4.42.01], with total respect to the mesh reference frame:

```
AFFE_CARA_ELEM (HULL = _F (ANGL_REP =  (α,β)  ))
```

It is built by has periodic concrete homogenization approach using the averaging method and it couples concrete ramming and periodic debonding between steel rebar and surrounding. It leads to has better modelling of the energy dissipation during loading cycles.

By construction, the DHRC model has comparable performance in terms of computational cost and numerical robustness with GLRC_DM model.

With restricted number of geometric and material characteristics are needed from which the whole set of model parameters are identified through year automatic numeric procedure performed there is Representative Volume Elements (RVE) of the RC punt.

Ace GLRC_DM model does, DHRC ones accounts for thermal strains, idealized in the punt thickness, see [R3.11.01].

1.3 Notations

In orthonormal Cartesian coordinate system is chosen so that covariant and counter-variable components are assimilated. Uppercase letters will refer generally to the macroscopic scale and lowercase ones to the microscopic scale. The simply contracted tensorial product will Be noted by has simple dowry “ . ” and the double one by two dowries “ : ” gold “ $\otimes$ ”. - Tensor components will Be given through subscripts relatively to the differential manifold used: Greek subscripts will set for integers ranging from 1 to 2 and Latin ones for integers ranging from 1 to 3.

2 Constitutive formulation of the law

2.1 Actual problem and modelling assumptions

We consider has concrete panel reinforced by two steel grids located one one side and the other of the middle planes of the punt. The thickness H of the punt is considered to side Be small compared to its overall dimensions L_1 and L_2, see Figure 2 - 1, and the grids are composed with has periodic pattern of natural periodicity along $\mathbf{e}_{x_1}$ and $\mathbf{e}_{x_2}$ directions of the same length order ace H. Moreover we consider space that external loading and inertia forces distributions are “smooth” with respect to the thickness H of the punt and restricted to the low frequencies arranges, ace usual for seismic studies. Thus, it is possible to define has Reference Volume Element (RVE), denoted hereafter by Ω, including both concrete and steel grids, whose side dimensions are l_1 and l_2, see Figure 2 - 1. We assumes that the side ratio of the dimensions l_1 however l_2 over

the dimensions L_1 however L_2 of the whole punt is of the same length order ace the ratio of the punt thickness H over its side dimensions.

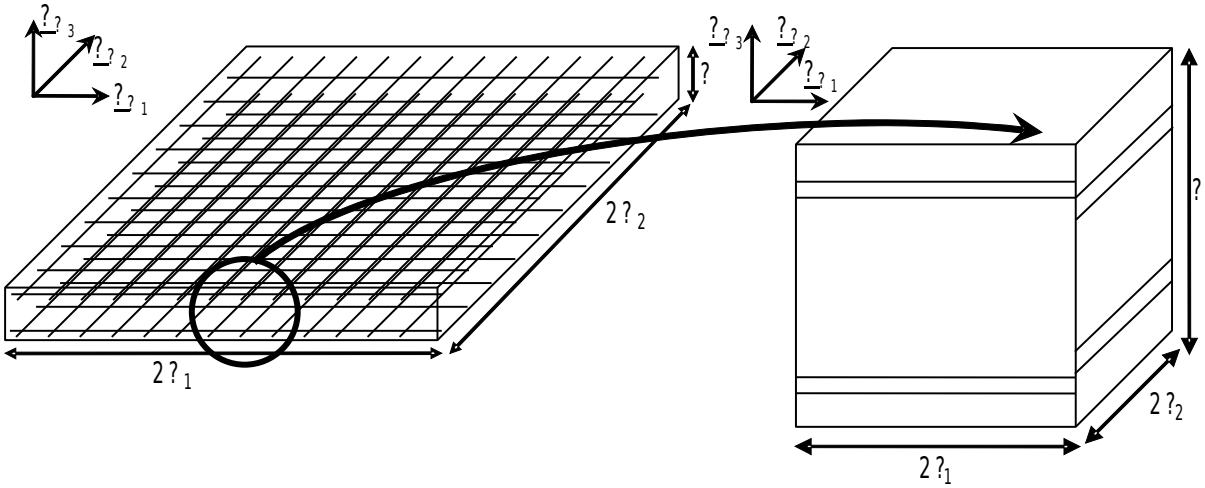

Figure 2.1-a : RVE Ω definition from the actual RC punt geometry.

We are interested in deriving year overall macroscopic constitutive punt relation and the previous geometrical characteristics lead custom to uses has multi-scale analysis gold has homogenization technical, ace it was already proposed in the literature for many decades. In the box where components are assumed to Be linear elastic, this multi-scale approach has been justified by using year asymptotic expansion method one three-dimensional elasticity equations. It leads to the well-known bi--dimensional linear Coils-Kirchhoff' S thin relative punt theory yew the dimensionless size of heterogeneities is of the same order that the slenderness of the solid, [bib16].

Both periodicity to say ctions $\mathbf{e}_{x_1}$ and $\mathbf{e}_{x_2}$, corresponding to steel grid rebar directions, will Be preferred directions for the after-effect of this document. The chosen microscopic coordinate system will Be the steel grid coordinate system $\left(O,\mathbf{e}_{x_1},\mathbf{e}_{x_2},\mathbf{e}_{x_3}\right)$, where $\mathbf{e}_{x_3}=\mathbf{e}_{X_3}$ and O is the center of the considersD RVE. Plane The $x_3=0$ is the mid-plane of the RVE.

Upper and lower faces of the RVE are assumed to Be free of load, see [bib16].
Given the fact that material considerations for the actual RC punt problem are complex, several simplifications cuts been proposed. Ace reported in Suquet' S work (Suquet, 1993), the essential properties of the macroscopic homogenised model are directly defined from average energetic quantities that are computed from microscopic corresponding ones in the RVE and from local sum optimization arguments associated to thermodynamic equilibrium – especially in the standard generalised materials context (Halphen & Nguyen, 1975). Therefore, it is believed that average quantities edge wrestling with has reasonable good agreement the overall behaviour of year actual RC punt, even yew the detail of microscopic phenomena is roughly idealised. Constitutive The hypothesis about materials and to their jump behaviours, needed to formulate the mathematical expression of the model are listed below with to their justifications

2.1.1 Materials behaviour in RVE Ω

Hyp 1. Steel is considered linear elastic, without irreversible plastic strains, ace we C not consider ultimate states of the RC punt. We indicates by $\mathbf{a}^s$ the corresponding elastic tensor.

Hyp 2. Concrete is considered elastic and damageable, according to the following constitutive model $\boldsymbol{\sigma}=\mathbf{a}^c(d):\boldsymbol{\varepsilon}$, d being has scalar variable ramming idealising distributed cracking. The

associated induced anisotropy is modelled through has suitable of definition $\mathbf{a}^c(d)$. Concrete rigidity tensor $\mathbf{a}^c(d)$ is defined by its initial undamaged been worth $\mathbf{a}^c(0)$, whose components are reduced by has decreasing convex ramming function $\xi(d)$. Give We will more details about the concrete constitutive model in section 4.2.

2.1.2 Steel-concrete interface in RVE Ω

Hyp 3. Concrete and steel rebar edge slide one one the other beyond has given threshold.
Hyp 4. Steel-concrete The jump status At interface is either sticking gold sliding. Normal separation is not allowed. We C not consider any interface elastic energy associated to the sliding motion.
Hyp 5. Steel-concrete relative The sliding, appearing after concrete ramming and concrete transmission of internal forces from to steel rebar, edge occur only in the two preferred directions $\mathbf{e}_{x_1}$ and $\mathbf{e}_{x_2}$ -- along longitudinal rebar. It edge differ whether considering the bar of the upper grid gold of the lower grid, thus allowing to take into account its consequence one the RC punt flexural behaviour. Let' S indicates by Γ_b the generic steel-concrete interfaces along $\mathbf{e}_{x_1}$ however $\mathbf{e}_{x_2}$.
Hyp 6. Orthogonal Steel rebar to the sliding direction -- i.e either perpendicular grid rebar but transverse rebar -- are considered to prevent relative sliding. Ace has consequence, steel-concrete sliding is periodical with has period equal to the spacing between two consecutive grid bars in the considered sliding direction. Side This defines the dimensions of the RVE Ω .

2.1.3 Non-uniform ramming in RVE Ω

Hyp 7. In order to the non-uniform ramming concrete distribution of along the steel rebar idealizes, concrete domain in concrete the RVE is in fact divided into two sub-domains associated respectively to sound and damaged one. Therefore, we define has whole RVE partition into two sub-domains Ω_{sd} and Ω_{dm} , respectively. The Γ_s interface between thesis two sub-domains is assumed to Be totally stuck.

Actually, concrete of the punt is not damaged in has uniform way in its volume. In order to idealizes this phenomenon, one should introduce has non-uniformly distributed variable ramming D in the whole RVE. Nevertheless, according to the Suquet' S work (Suquet, 1987), this non-uniformity of the microscopic internal variable field leads to the necessity to consider year infinity number of macroscopic internal variable At each macroscopic material not. This resulting prevents the practical uses of the macroscopic standard generalised model that would result from the chosen microscopic ones. However, still according to (Suquet, 1987), it is possible to reduce this number of internal variable to has finite one yew it edge Be demonstrated that thesis internal variable are uniform gold piecewise uniform gold more generally described by has vector space of finite dimension. Standard The generalised character of the macroscopic model is obtained from the microscopic scale behaviours thanks to the usual properties of Caratheodory' S functions of Convex Analysis. Thus, yew such has chosen set of internal variable edge re-press the actual material state in the RVE, with has sufficient approximation dismantles, it is possible to build has macroscopic standard generalised model with has finite number of macroscopic internal variable. In our studies, order to restrict the number of macroscopic internal variable, we decided to define only one microscopic internal variable D for ramming, considered ace piecewise uniformly distributed inside the different whole RVE and two sets of materials representing two states of ramming in concrete located in sub-domains Ω_{sd} and Ω_{dm} . This distribution of microscopic ramming allows in has simple way the representation of the “tension-stiffening” effect (Combescure and al., 2013). The been worth of microscopic and macroscopic internal variable d and D are then equated, for the sake of simplicity, without losing any generality, since the only to subdue is the actual been worth of the respective elastic stiffness tensors.

Hyp 8 . In order to take into account the has priori non-uniform ramming in the RVE thickness, two ramming variables will Be set up corresponding to the piecewise ramming in the upper and lower halves of the RVE.

$$d = \begin{cases} d_1 \ if \ \ x_3 \geqslant 0 \\ d_2 \ if \ \ x_3 < 0 \end{cases} \tag{2.1-1}$$

This leads to has macroscopic ramming also decomposed into two variable macroscopic D^1 and D^2 .

Variable This strong hypothesis of microscopic ramming stepped distribution is about to re-presses common experimental observations during oven points bending tests one RC punts: aces opened in tension shares of the punt appear and propagate dynamically quasi-instantaneously through about the half of thickness. This ace adequate propagation time scale is much smaller than the one considered in seismic analysis and it is then to separate ramming into two variable depending one the position x_3 in the punt thickness. The distinction between those two ramming steps is chosen to Be exact At the middle plane Γ_m of the punt, being the perfectly stuck interface between upper and lower halves of the RVE. This strong concrete approximation is in accordance with reinforced design standards and regulations where it is advised to consider only half of the concrete section, for bending design, e.g. (CEB-FIP Model Codes 1990.1993). In the after-effect, microscopic and macroscopic ramming variables will Be respectively noted d^ζ and D^ζ depending variable yew the considered is the one of the upper ($\zeta = 1$) however lower ($\zeta = 2$) half of the RVE, see Figure 2.1.3-a.

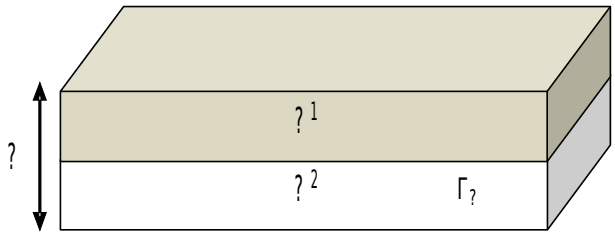

Figure 2.1.3-a : Variable Depiction of the microscopic ramming d discretised in the RVE thickness.

Ounce admitted this distinction between upper and lower halves of the RVE, sub-domains Ω_i ($i = sd\,,dm$, according to the ramming status) and steel-concrete interfaces Γ_b must Be Split respectively in Ω_i^1 , Ω_i^2 and Γ_b^1 , Γ_b^2 . Interfaces Γ_b^1 and Γ_b^2 will then Be denoted by Γ_b^ζ , with $\zeta = 1,2$.

2.1.4 Steel-concrete Non-uniform debonding in RVE Ω

Let' S consider, in the RVE sketched At Figure 2.1.4-a, that sliding edge occur At steel-concrete interfaces Γ_b^ζ along the $\mathbf{e}_{x_1}$ however $\mathbf{e}_{x_2}$ directions.

The shapes of sliding functions $\boldsymbol{\eta}^\zeta(x)$ At the interfaces Γ_b^ζ should result from the mechanical energy minimization and then depend one the loading history in the RVE. Thus, they remain unknown before the introduction of macroscopic loading over the whole punt and boat Be determined a priori. Ace has consequence, the choice is made to prescribe *a priori* shapes for thesis functions in order to process conveniently to the periodic homogenization with has limited number variable of. Moreover, ace well ace ramming has been Be chosen piecewise uniform inside the whole links concealment, it appears necessary to define sliding along each rebar from one only parameter per direction and per grid. Several possibilities edge then Be chosen: either the tangential displacement gap corresponding to the sliding is constant, either jump-stress induced by this sliding are. According to (Marti and al. 1998), debonding induced stress are assumed to constant Be piecewise.

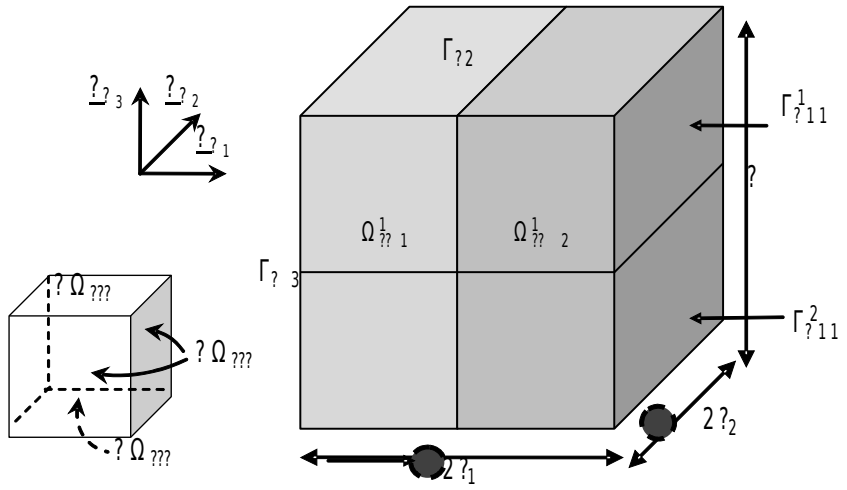

Figure 2.1.4-a : Depiction of the sub-domains within the RVE thickness.

Hyp 9 . Considering the previous observation from (Marti et al. 1998), has bilinear sliding function (sketched At Figure 2.1.4-b) is chosen – corresponding to piecewise jump stress At the interface Γ_b^ζ . This sliding function is only parameterised by its amplitude, its periodicity being fixed by the one of the RVE.

Hyp 10. Steel-concrete Moreover, it will Be considered that sliding vector in the $\mathbf{e}(x_\alpha)$ direction, denoted by $\boldsymbol{\eta}_\alpha^\zeta$, depend only one the x_α coordinate: it takes the same been worth At any not located At the steel-concrete interface Γ_b^ζ for has given x_α . Let' S indicates by $\hat{\eta}_\alpha^\zeta(x_\alpha)$ the sliding function of unitary amplitude for the $\mathbf{e}(x_\alpha)$ direction. Ace has result: $\hat{\boldsymbol{\eta}}_\alpha^\zeta(x_\alpha)=E_\alpha^{\eta\zeta}.\hat{\eta}_\alpha^\zeta(x_\alpha).\mathbf{e}(x_\alpha)$, $E_\alpha^{\eta\zeta}$ being its amplitude. Moreover, we observes that $\frac{1}{l_\alpha}\int_{-l_\alpha}^{l_\alpha}\hat{\eta}_\alpha^\zeta dx_\alpha=1$.

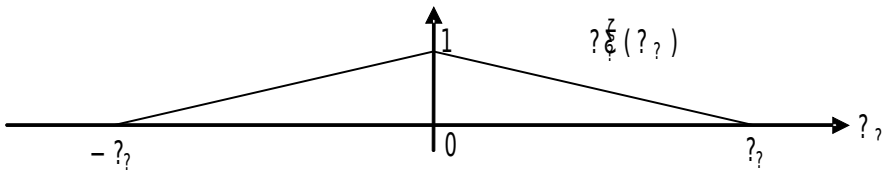

Figure 2.1.4-b : Periodic sliding shape function distribution $\hat{\eta}_\alpha$ along the $\mathbf{e}(x_\alpha)$ direction with unitary amplitude in the RVE.

2.1.5 Overall strains measures and macroscopic state variable one RVE Ω

Now, according to the previous selection of phenomena to Be idealised, we cuts to define has set of independent state variable, whitebait to describe the mechanical state evolutions of structural the RC punt element At macro-scale the. First of all, the local microscopic displacement field $\mathbf{u}$ in the RVE $\Omega=\cup\Omega_i^\zeta$ ($i=sd,dm$ in concrete, and $i=s$ in steel rebar) is Split into has regular share

$\mathbf{u}^r$ and has discontinuous one $\mathbf{u}^d$, associated with the debonding relative displacement defined by the $\boldsymbol{\eta}_\alpha^\zeta$ functions (Hyp 10) At the steel-concrete interfaces Γ_b^ζ .

The overall strains measures defined ace the result of the homogenization of thin punt are the following mean surface strain tensors of second order, according to Kirchhoff-Love' S kinematics (Caillerie & Nedelec, 1984): macroscopic membrane strain tensor $\mathbf{E}$, whose components are denoted by $E_{\alpha\beta}$, and macroscopic bending strain tensor $\mathbf{K}$ (curvature At first order), whose components are denoted by $K_{\alpha\beta}$. Ace we indicates by $\boldsymbol{\varepsilon}(\mathbf{u})$ the microscopic strain tensor associated to local displacement field $\mathbf{u}$ in the RVE $\Omega = \cup\Omega_i^\zeta$, the components of $\mathbf{E}$ and $\mathbf{K}$ tensors are defined by the following average linear operators from the regular share $\mathbf{u}^r$ of the displacement field:

$$\begin{cases} E_{\alpha\beta} = \dfrac{1}{|\Omega|}\int_{\cup\Omega_i^\zeta} \varepsilon_{\alpha\beta}(\mathbf{u}^r)\, d\,\Omega \\ K_{\alpha\beta} = \dfrac{12}{H^2|\Omega|}\int_{\cup\Omega_i^\zeta} -x_3\,\varepsilon_{\alpha\beta}(\mathbf{u}^r)\, d\,\Omega \end{cases} \tag{2.1-2}$$

In the after-effect, the following notation $<\cdot>_\Omega = \dfrac{1}{|\Omega|}\int_{\cup\Omega_i^\zeta}\cdot\, dV$ stands for the average been worth of the considered field in the RVE. We edge easily observes that the expressions in (2 1-2) encompass the usual definition for homogeneous punt kinematics.

We must now deal with the non-regular share $\mathbf{u}^d$ of the displacement field in the RVE. In the after-effect $[\![.]\!]$ stands for the jump operator one the steel-concrete interface. So, we define the macroscopic sliding strain tensor $E^{\eta\zeta}$ ace the average of sliding one each steel-concrete interface Γ_b^ζ . First, we observes that the contribution of discontinuous displacement $\mathbf{u}^d$ to the macroscopic strain tensors vanishes, due to Hyp 4 and Hyp 10 (Andrieux and al., 1986):

$$\frac{1}{|\Omega|}\int_{\Gamma_b^\zeta}[\![\mathbf{u}^d]\!]\otimes^s\mathbf{n}\,dS = 0 \quad ; \quad \frac{1}{|\Omega|}\int_{\Gamma_b^\zeta} x_3.[\![\mathbf{u}^d]\!]\otimes^s\mathbf{n}\,dS = 0 \tag{2.1-3}$$

where $\mathbf{n}$ is the outward normal At the steel-concrete interface Γ_b^ζ and $\otimes^s$ stands for the symmetrised dyadic tensor product. According to Hyp 4, the displacement discontinuity $[\![\mathbf{u}^d]\!] = \boldsymbol{\eta}^\zeta(\mathbf{x})$ At the interface Γ_b^ζ does not include any opening gold separation in the $\mathbf{n}$ direction, goal only tangential sliding $\boldsymbol{\eta}_\alpha^\zeta$. Extending the proposed definition by (Combescure and al., 2013), the components of $E^{\eta\zeta}$ are:

$$E_{\alpha\alpha}^{\eta\zeta} = \frac{1}{|\Omega|}\int_{\Gamma_b^\zeta}\left([\![\mathbf{u}^d]\!].\mathbf{e}_{x_\alpha}\right).\mathbf{e}_{x_\alpha}\otimes^s\mathbf{e}_{x_\alpha}\,dS \tag{2.1-4}$$

Indeed, the only non-zero components of tensor $\mathbf{E}^{\eta\zeta}$ are $E_{\alpha\alpha}^{\eta\zeta}$. Vector $\mathbf{E}^{\eta\zeta}$ will then more conveniently Be considered in the following ace has first-order tensor of the punt mean surface, whose components are denoted by $E_\alpha^{\eta\zeta}$.

Primal The macroscopic state variable associated to the DHRC proposed model are then: membrane strains $\mathbf{E}$ and bending strains $\mathbf{K}$ tensors, ramming variables D^ζ one upper and lower halves of the homogenised punt, sliding strain $\mathbf{E}^{\eta\zeta}$ vectors one upper and lower grids. Thesis

variables will Be used to define state functions, ace the macroscopic free energy density $W\left(\mathbf{E},\mathbf{K},D^{\zeta},\mathbf{E}^{\eta\zeta}\right)$.

3 Weak forms of the auxiliary problems and homogenised model

3.1 Room auxiliary problems

In order to given the macroscopic constitutive relation, we cuts to establish the relation between microscopic fields and macroscopic ones, for various fixed been worth of internal state variable. This relation concerns displacements fields, strain work density and dissipation potentials.

At the RVE level, ace has consequence of equalities (2.1-2) and (2.1-4), let' S introduce two microscopic auxiliary displacement fields:

- "elastic" displacement fields in membrane χ and bending ξ corresponding to has given non-zero macroscopic strain tensor -- $\mathbf{E}$ in membrane and $\mathbf{K}$ in bending -- with zero sliding ($\mathbf{E}^{\eta\zeta}=\mathbf{0}$);
- "sliding" displacement fields $\chi^{\eta_\alpha^\zeta}$, corresponding to vanishing macroscopic strains ($\mathbf{E}=\mathbf{0}$, $\mathbf{K}=\mathbf{0}$) corresponding to has given sliding function $\eta_\alpha^\zeta(x_\alpha)$ however equivalently has given $E_\alpha^{\eta\zeta}$, ace gives in (Andrieux et al. 1986; Thought & Kondo 2001).

Hence the microscopic displacement field $\mathbf{u}$, solution of the local boundary been worth problem in the RVE, edge Be decomposed ace follows (omitting intentionally the solid motion to shorten the expression):

$$\begin{cases} u_\alpha(\mathbf{x}) = E_{\alpha\beta}\,x_\beta - K_{\alpha\beta}\,x_\beta x_3 + E_{\beta\gamma}\,\chi_\alpha^{\beta\gamma}(\mathbf{x}) + K_{\beta\gamma}\,\xi_\alpha^{\beta\gamma}(\mathbf{x}) + E_\beta^{\eta\zeta}\,\chi_\alpha^{\eta_\beta^\zeta}(\mathbf{x}) \\ u_3(\mathbf{x}) = E_{\beta\gamma}\,\chi_3^{\beta\gamma}(\mathbf{x}) + K_{\beta\gamma}\,\xi_3^{\beta\gamma}(\mathbf{x}) + E_\beta^{\eta\zeta}\,\chi_3^{\eta_\beta^\zeta}(\mathbf{x}) \end{cases} \tag{3.1-1}$$

We define the following functional spaces for displacement fields in Ω (Caillerie & Nedelec, 1984):

$$U_{ad}^0 = \left\{ \mathbf{v} / \mathbf{v}\ periodic \text{ in } x_1 \text{ and } x_2, \mathbf{v}\ continuous\ on\ \Gamma_b^1 \cup \Gamma_b^2 \cup \Gamma_s \right\} \tag{3.1-2}$$

and:

$$U_{ad}^{\alpha\rho} = \left\{ \mathbf{v} / \mathbf{v}\ periodic \text{ in } x_1 \text{ and } x_2, \mathbf{v}\ continuous\ on\ \Gamma_s, \mathbf{v}_n\ continuous \text{ and } \left[\left[\mathbf{v}_T\right]\right] = E_\alpha^{\eta\rho}\hat{\eta}_\alpha^\rho(x_\alpha) \right. \tag{3.1-3}$$

Remark 1:

We edge easily prove that $\langle \boldsymbol{\varepsilon}(\mathbf{v})\rangle_\Omega = \langle x_3\,\boldsymbol{\varepsilon}(\mathbf{v})\rangle_\Omega = 0$ for any $\mathbf{v}$ in U_{ad}^0 had to the periodicity and, using equations (2-3), that $\langle \boldsymbol{\varepsilon}(\mathbf{v})\rangle_\Omega = \langle x_3\,\boldsymbol{\varepsilon}(\mathbf{v})\rangle_\Omega = 0$ for any $\mathbf{v}$ in $U_{ad}^{\alpha\rho}$.

Strain work density At the macroscopic scale is obtained by the exploitation of extended Hill-Mandel' S principle (Sanchez-Palencia, 1987; Suquet, 1987), extended to thin punt put by (Caillerie & Nedelec, 1984). Generalised resulting stresses, dual of the primal overall variable strain $\mathbf{E}$, $\mathbf{K}$, and $\mathbf{E}^{\eta\zeta}$ are respectively denoted by: $\mathbf{N}$, $\mathbf{M}$ and debonding stress vector $\boldsymbol{\Sigma}^{\eta\zeta}$. Macroscopic strain work balances reads:

$$\mathbf{N}:\mathbf{E}+\mathbf{M}:\mathbf{K}+\mathbf{\Sigma}^{\eta\zeta}.\mathbf{E}^{\eta\zeta}=\frac{H}{|\Omega|}\int_{\cup\Omega_i^\zeta}\boldsymbol{\sigma}_{pq}:\boldsymbol{\varepsilon}_{pq}(\mathbf{u})\,d\,\Omega \tag{3.1-4}$$

Introducing Hyp 1 and Hyp 2 assumptions about the material behaviours within the RVE, the overall strain variable definition (cf section 2.1.5), and the microscopic displacement field decomposition (3-1.1) in the strain work balances (3.1-4), microscopic periodic auxiliary displacement fields satisfy the following ten linear elastic auxiliary problems, defined in the RVE, the ramming state d^ζ being fixed (subscript $k=c$ however s, for concrete gold steel):

Find $\boldsymbol{\chi}_{\alpha\beta}\in U_{ad}^0$ so that:
$\int_{\cup\Omega_i^\zeta}\varepsilon_{pq}(\boldsymbol{\chi}^{\alpha\beta}):a_{pqrs}^k(d^\zeta):\varepsilon_{rs}(\mathbf{v})\,d\,\Omega\;=\;-\int_{\cup\Omega_i^\zeta}a_{\alpha\beta rs}^k(d^\zeta):\varepsilon_{rs}(\mathbf{v})\,d\,\Omega\quad\forall\;\mathbf{v}\in U_{ad}^0$

Find $\boldsymbol{\xi}_{\alpha\beta}\in U_{ad}^0$ so that:
$\int_{\cup\Omega_i^\zeta}\varepsilon_{pq}(\boldsymbol{\xi}^{\alpha\beta}):a_{pqrs}^k(d^\zeta):\varepsilon_{rs}(\mathbf{v})\,d\,\Omega\;=\;+\int_{\cup\Omega_i^\zeta}x_3:a_{\alpha\beta rs}^k(d^\zeta)\,\varepsilon_{rs}(\mathbf{v})\,d\,\Omega\quad\forall\;\mathbf{v}\in U_{ad}^0$ (3.1-5)

Find $\boldsymbol{\chi}^{\eta_\alpha^\zeta}\in U_{ad}^{\alpha\rho}$ so that:
$\int_{\cup\Omega_i^\zeta}\varepsilon_{pq}(\boldsymbol{\chi}^{\eta_\alpha^\rho}):a_{pqrs}^k(d^\zeta):\varepsilon_{rs}(\mathbf{v}-\boldsymbol{\chi}^{\eta_\alpha^\rho})\,d\,\Omega\;=\;0\quad\forall\;\mathbf{v}\in U_{ad}^{\alpha\rho}$

i.e. three problems in membrane, three ones in bending and the last oven associated to sliding.

Thus, any microscopic displacement field $\mathbf{u}$ edge Be expressed with the help of the previous ten auxiliary fields, by linear superposition (3-1.1). Thanks to thesis results, macroscopic strain work density edge Be written in terms of macroscopic state variable.

3.2 Macroscopic homogenised model

In the following we shall adopt the notation: $\langle\langle\cdot\rangle\rangle_\Omega=\frac{H}{|\Omega|}\int_{\cup\Omega_i^\xi}\cdot\,dV$ for the average been worth per punt surface links of the considered field in the RVE Ω, H being the punt thickness, identical to the one of the RVE. The macroscopic homogenised model is obtained through the usual exploitation of extended Hill-Mandel' S principle applied to get the macroscopic Helmoltz' free energy surface density $W(\mathbf{E},\mathbf{K},D^\zeta,\mathbf{E}^{\eta\zeta})$ of the constitutive punt model. This equates the average $\langle\langle w^i(\varepsilon(\mathbf{u}),d^\zeta)\rangle\rangle_\Omega$ of the microscopic free energy densities in the RVE, where, accordingly to assumptions Hyp 1 and Hyp 2:

$$w^k(\boldsymbol{\varepsilon}(\mathbf{u}),d^\zeta)=\frac{1}{2}\boldsymbol{\varepsilon}(\mathbf{u}):a^k(d^\zeta):\boldsymbol{\varepsilon}(\mathbf{u}) \tag{3.2-1}$$

with $k=c$ however s, for concrete gold steel. In the following, we will omitted this superscript to ease writing.

After solving of the ten elastic linear independent auxiliary problems (3-1.5) (in practice by numerical analysis), the macroscopic free energy density edge Be expressed ace follows, using expressions (3-1.1), depending one the macroscopic strain tensors $\mathbf{E}$, $\mathbf{K}$, and one the macroscopic ramming and sliding internal variable D and $\mathbf{E}^{\eta\zeta}$, respectively, given with fixed been worth:

$$\begin{aligned}
2W(\mathbf{E},\mathbf{K},\mathbf{D},\mathbf{E}^{\eta}) = {} & \mathbf{E}:\langle\langle a(d)\rangle\rangle_{\Omega}:\mathbf{E} - E_{\alpha\beta}\langle\langle \varepsilon(\boldsymbol{\chi}^{\alpha\beta}):a(d):\varepsilon(\boldsymbol{\chi}^{\gamma\delta})\rangle\rangle_{\Omega}E_{\gamma\delta} \\
& -2\,\mathbf{E}:\langle\langle x_3.a(d)\rangle\rangle_{\Omega}:\mathbf{K} - 2\,E_{\alpha\beta}\langle\langle \varepsilon(\boldsymbol{\chi}^{\alpha\beta}):a(d):\varepsilon(\boldsymbol{\xi}^{\gamma\delta})\rangle\rangle_{\Omega}K_{\gamma\delta} \\
& +\mathbf{K}:\langle\langle x_3^2.a(d)\rangle\rangle_{\Omega}:\mathbf{K} - K_{\alpha\beta}\langle\langle \varepsilon(\boldsymbol{\xi}^{\alpha\beta}):a(d):\varepsilon(\boldsymbol{\xi}^{\gamma\delta})\rangle\rangle_{\Omega}K_{\gamma\delta} \\
& +2\,\mathbf{E}:\langle\langle a(d):\varepsilon(\boldsymbol{\chi}^{\eta_\gamma^\zeta})\rangle\rangle_{\Omega}\mathbf{E}_{\gamma}^{\eta\zeta} \\
& -2\,\mathbf{K}:\langle\langle x_3.a(d):\varepsilon(\boldsymbol{\chi}^{\eta_\gamma^\zeta})\rangle\rangle_{\Omega}\mathbf{E}_{\gamma}^{\eta\zeta} \\
& +E_{\alpha}^{\eta\rho}\langle\langle \varepsilon(\boldsymbol{\chi}^{\eta_\alpha^\rho}):a(d):\varepsilon(\boldsymbol{\chi}^{\eta_\gamma^\zeta})\rangle\rangle_{\Omega}\mathbf{E}_{\gamma}^{\eta\zeta}
\end{aligned} \tag{3.2-2}$$

Therefore, we edge identify three homogenised behaviour tensors $\mathbf{A}$, $\mathbf{B}$, $\mathbf{C}$ of respectively fourth, third and second order, defined in the tangent planes of the punt ace:

$$\begin{aligned}
& 2W(\mathbf{E},\mathbf{K},\mathbf{D},\mathbf{E}^{\eta}) = \\
& \begin{pmatrix}\mathbf{E}\\ \mathbf{K}\end{pmatrix}:\begin{pmatrix}\mathbf{A}^{mm}(\mathbf{D}) & \mathbf{A}^{mf}(\mathbf{D})\\ \mathbf{A}^{fm}(\mathbf{D}) & \mathbf{A}^{ff}(\mathbf{D})\end{pmatrix}:\begin{pmatrix}\mathbf{E}\\ \mathbf{K}\end{pmatrix} + 2\begin{pmatrix}\mathbf{E}\\ \mathbf{K}\end{pmatrix}:\begin{pmatrix}\mathbf{B}^{m\zeta}(\mathbf{D})\\ \mathbf{B}^{f\zeta}(\mathbf{D})\end{pmatrix}.\mathbf{E}^{\eta\zeta} + \mathbf{E}^{\eta\rho}.C^{\rho\zeta}(\mathbf{D}).\mathbf{E}^{\eta\zeta}
\end{aligned} \tag{3.2-3}$$

in which pure membrane (mm), pure bending (ff) and membrane-bending (mf) terms are particularised:

$$\begin{aligned}
A^{mm}_{\alpha\beta\gamma\delta}(\mathbf{D}) &= \langle\langle a_{\alpha\beta\gamma\delta}(d)\rangle\rangle_{\Omega} - \langle\langle \varepsilon_{ij}(\boldsymbol{\chi}^{\alpha\beta}):a_{ijkl}(d):\varepsilon_{kl}(\boldsymbol{\chi}^{\gamma\delta})\rangle\rangle_{\Omega} \\
&= \langle\langle a_{\alpha\beta\gamma\delta}(d)\rangle\rangle_{\Omega} + \langle\langle a_{\alpha\beta rs}(d):\varepsilon_{rs}(\boldsymbol{\chi}^{\gamma\delta})\rangle\rangle_{\Omega}
\end{aligned} \tag{3.2-4}$$

$$\begin{aligned}
A^{mf}_{\alpha\beta\gamma\delta}(\mathbf{D}) &= -\langle\langle x_3.a_{\alpha\beta\gamma\delta}(d)\rangle\rangle_{\Omega} - \langle\langle \varepsilon_{ij}(\boldsymbol{\chi}^{\alpha\beta}):a_{ijkl}(d):\varepsilon_{kl}(\boldsymbol{\xi}^{\gamma\delta})\rangle\rangle_{\Omega} = A^{fm}_{\alpha\beta\gamma\delta}(\mathbf{D}) \\
&= -\langle\langle x_3.a_{\alpha\beta\gamma\delta}(d)\rangle\rangle_{\Omega} + \langle\langle a_{\alpha\beta rs}(d):\varepsilon_{rs}(\boldsymbol{\xi}^{\gamma\delta})\rangle\rangle_{\Omega} \\
&= -\langle\langle x_3.a_{\alpha\beta\gamma\delta}(d)\rangle\rangle_{\Omega} - \langle\langle x_3.a_{\gamma\delta rs}(d):\varepsilon_{rs}(\boldsymbol{\chi}^{\alpha\beta})\rangle\rangle_{\Omega}
\end{aligned} \tag{3.2-5}$$

$$\begin{aligned}
A^{ff}_{\alpha\beta\gamma\delta}(\mathbf{D}) &= \langle\langle x_3^2.a_{\alpha\beta\gamma\delta}(d)\rangle\rangle_{\Omega} - \langle\langle \varepsilon_{ij}(\boldsymbol{\xi}^{\alpha\beta}):a_{ijkl}(d):\varepsilon_{kl}(\boldsymbol{\xi}^{\gamma\delta})\rangle\rangle_{\Omega} \\
&= \langle\langle x_3^2.a_{\alpha\beta\gamma\delta}(d)\rangle\rangle_{\Omega} - \langle\langle x_3.a_{\alpha\beta rs}(d):\varepsilon_{rs}(\boldsymbol{\xi}^{\gamma\delta})\rangle\rangle_{\Omega}
\end{aligned} \tag{3.2-6}$$

$$B^{m\zeta}_{\alpha\beta\gamma}(\mathbf{D}) = \langle\langle a_{\alpha\beta kl}(d):\varepsilon_{kl}(\boldsymbol{\chi}^{\eta_\gamma^\zeta})\rangle\rangle_{\Omega} \tag{3.2-7}$$

$$B^{f\zeta}_{\alpha\beta\gamma}(\mathbf{D}) = -\langle\langle x_3.a_{\alpha\beta kl}(d):\varepsilon_{kl}(\boldsymbol{\chi}^{\eta_\gamma^\zeta})\rangle\rangle_{\Omega} \tag{3.2-8}$$

$$C^{\rho\zeta}_{\alpha\gamma}(\mathbf{D}) = \langle\langle \varepsilon_{ij}(\boldsymbol{\chi}^{\eta_\alpha^\rho}):a_{ijkl}(d):\varepsilon_{kl}(\boldsymbol{\chi}^{\eta_\gamma^\zeta})\rangle\rangle_{\Omega} \tag{3.2-9}$$

Remark 2:

> *First terms in the expressions (3.2-4-6) corresponds to the mixture rule; the second terms edge Be equivalently expressed using the variational formulations (3.1-5) ace reported young stag. Moreover, resulting from the symmetries of elastic tensor has, we note directly from thesis expressions the following symmetries:* $A^{mm}_{\alpha\beta\gamma\delta} = A^{mm}_{\gamma\delta\alpha\beta}$, $A^{ff}_{\alpha\beta\gamma\delta} = A^{ff}_{\gamma\delta\alpha\beta}$, $A^{mf}_{\alpha\beta\gamma\delta} = A^{mf}_{\gamma\delta\alpha\beta}$, $B^{m\zeta}_{\alpha\beta\gamma} = B^{m\zeta}_{\beta\alpha\gamma}$, $B^{f\zeta}_{\alpha\beta\gamma} = B^{f\zeta}_{\beta\alpha\gamma}$, $C^{\rho\rho}_{\alpha\gamma} = C^{\rho\rho}_{\gamma\alpha}$.

Ace expected, this free energy density W has major symmetry for membrane-bending terms. Moreover, it includes has coupling term $\mathbf{B}$ between generalised strain tensors and jump sliding

vectors that depend one ramming and hence strongly standard couples both of internal state variable (ramming and sliding).

Remark 3:

The free energy density (3.2-3) edge also Be written equivalently ace:

$$2W\left(\mathbf{E},\mathbf{K},\mathbf{D},\mathbf{E}^{\eta}\right)=\left[\begin{pmatrix}\mathbf{E}\\ \mathbf{K}\end{pmatrix}+\begin{pmatrix}\mathbf{Q}^{m\zeta}(\mathbf{D})\\ \mathbf{Q}^{f\zeta}(\mathbf{D})\end{pmatrix}.\mathbf{E}^{\eta\zeta}\right]:\begin{pmatrix}\mathbf{A}^{mm}(\mathbf{D}) & \mathbf{A}^{mf}(\mathbf{D})\\ \mathbf{A}^{fm}(\mathbf{D}) & \mathbf{A}^{ff}(\mathbf{D})\end{pmatrix}:\left[\begin{pmatrix}\mathbf{E}\\ \mathbf{K}\end{pmatrix}+\begin{pmatrix}\mathbf{Q}^{m\zeta}(\mathbf{D})\\ \mathbf{Q}^{f\zeta}(\mathbf{D})\end{pmatrix}.\mathbf{E}^{\eta\zeta}\right]+\mathbf{E}^{\eta\rho}.\mathbf{P}^{\rho\zeta}(\mathbf{D}).\mathbf{E}^{\eta\zeta} \quad (3.2\text{-}10)$$

where: $\mathbf{Q}^{\zeta}(\mathbf{D})=\mathbf{A}^{(-1)}(\mathbf{D}):\mathbf{B}^{\zeta}(\mathbf{D})$. and $\mathbf{P}^{\rho\zeta}(\mathbf{D})=\mathbf{C}^{\rho\zeta}(\mathbf{D})-(\mathbf{B}^{\rho})^{T}(\mathbf{D}):\mathbf{A}^{(-1)}(\mathbf{D}):\mathbf{B}^{\zeta}(\mathbf{D})$

This expression emphasises the existence in the presented free energy density of has coupling term between ramming and sliding through year inelastic strain $\mathbf{E}^{IR}(\mathbf{D})=\begin{pmatrix}\mathbf{Q}^{m\zeta}(\mathbf{D})\\ \mathbf{Q}^{f\zeta}(\mathbf{D})\end{pmatrix}.\mathbf{E}^{\eta\zeta}$ depending one ramming variables. Ace observed in (Combescure and al., 2013), this constitutes has feature that is justified by the homogenization constitutive procedure from microscopic behaviour. Constitutive It makes this model differ from usual models coupling ramming and plasticity (Nedjar, 2001; Chaboche, 2003; Krätzig & Pölling, 2004; Shao and al., 2006; Richard & Ragueneau, 2013…) where it is more common to refer to year inelastic residual strain $\mathbf{E}^{IR}$ independent of ramming. Present Conversely, the feature edge Be found in the work of (Andrieux and al., 1986), for the same reason, through homogenization process.

Remark 4:

Expression (3.2-2) of the free energy density has natural generalization, dedicated to punt structures, of the one-dimensional formulation proposed by (Combescure, Dumontet, & Voldoire, 2013) and remembered young stag:
$\Phi(E,D,E^{\eta})=(A(D).E^{2})/2-B(D).E.E^{\eta}+(C(D).E^{\eta 2})/2$.

Remark 5:

Possible It is to prove that coupling tensor $\mathbf{B}$ *is equal to zero ace long ace the microscopic stiffness tensor* $\mathbf{a}(d)$ *is identical in both sub-domains* Ω_{sd} *and* Ω_{dm} *, see section 7.3, meaning that it deals with the box where ramming is uniformly distributed At microscopic scale, in the whole RVE. This was observed in (Combescure and al., 2013) too and confirms experimental fact concerning the concrete tension-stiffening effect gold stress transfer from rebar to induced by the non-uniformity of ramming distribution local At scale*.

According to the theoretical framework of the Thermodynamic of Irreversible Process, the free energy density (*3.2-2*) edge Be differentiated to obtain the following thermodynamic forces and state laws:

- Resulting stresses one the homogenised punt (membrane and bending):

$$\mathbf{N}=\frac{\partial W}{\partial \mathbf{E}}=\begin{bmatrix}\mathbf{A}^{mm}(\mathbf{D}) & \mathbf{A}^{mf}(\mathbf{D})\end{bmatrix}:\begin{pmatrix}\mathbf{E}\\ \mathbf{K}\end{pmatrix}+\mathbf{B}^{m\zeta}(\mathbf{D}).\mathbf{E}^{\eta\zeta} \quad (3.2\text{-}11)$$

$$\mathbf{M}=\frac{\partial W}{\partial \mathbf{K}}=\begin{bmatrix}\mathbf{A}^{fm}(\mathbf{D}) & \mathbf{A}^{ff}(\mathbf{D})\end{bmatrix}:\begin{pmatrix}\mathbf{E}\\ \mathbf{K}\end{pmatrix}+\mathbf{B}^{f\zeta}(\mathbf{D}).\mathbf{E}^{\eta\zeta} \quad (3.2\text{-}12)$$

Using Voigt' S notation for matrices, this reads:

$$\begin{pmatrix} A^{ff}_{xxyy} & A^{ff}_{xxxy} \\ A^{ff}_{yyyy} & A^{ff}_{yyxy} \\ & A^{ff}_{xyxy} \end{pmatrix} \begin{pmatrix} \kappa_{xx} \\ \kappa_{yy} \\ \kappa_{xy} \end{pmatrix} \cdot \begin{pmatrix} B^{f1}_{xx\,x} & B^{f1}_{xx\,y} & B^{f2}_{xx\,x} & B^{f2}_{xx\,y} \\ B^{f1}_{yy\,x} & B^{f1}_{yy\,y} & B^{f2}_{yy\,x} & B^{f2}_{yy\,y} \\ B^{f1}_{xy\,x} & B^{f1}_{xy\,y} & B^{f2}_{xy\,x} & B^{f2}_{xy\,y} \end{pmatrix} \begin{pmatrix} E^{\eta 2}_{x} \\ E^{\eta 2}_{y} \end{pmatrix} \tag{3.2-13}$$

- Macroscopic energy disastrous restitution G^{ρ} :

$$G^{\rho} = -\frac{\partial W}{\partial D^{\rho}} \tag{3.2-14}$$

- Macroscopic debonding stress vector $\mathbf{\Sigma}^{\eta\zeta}$:

$$\mathbf{\Sigma}^{\eta\zeta} = -\frac{\partial W}{\partial \mathbf{E}^{\eta\zeta}} = -\begin{pmatrix} \mathbf{B}^{m\zeta}(\mathbf{D}) \\ \mathbf{B}^{f\zeta}(\mathbf{D}) \end{pmatrix} : \begin{bmatrix} \mathbf{E} & \mathbf{K} \end{bmatrix} - \mathbf{C}^{\rho\zeta}(\mathbf{D}) . \mathbf{E}^{\eta\rho} \tag{3.2-15}$$

Using Voigt' S notation for matrices, with (x, y) denoting the local rebar axes and $(1,2)$ the upper and lower steel grids, this reads:

$$\begin{pmatrix} \mathbf{\Sigma}^{\eta 1}_{x} \\ \mathbf{\Sigma}^{\eta 1}_{y} \\ \mathbf{\Sigma}^{\eta 2}_{x} \\ \mathbf{\Sigma}^{\eta 2}_{y} \end{pmatrix} = -\begin{pmatrix} B^{m1}_{xx\,x} & B^{m1}_{yy\,x} & B^{m1}_{xy\,x} & B^{f1}_{xx\,x} & B^{f1}_{yy\,x} & B^{f1}_{xy\,x} \\ B^{m1}_{xx\,y} & B^{m1}_{yy\,y} & B^{m1}_{xy\,y} & B^{f1}_{xx\,y} & B^{f1}_{yy\,y} & B^{f1}_{xy\,y} \\ B^{m2}_{xx\,x} & B^{m2}_{yy\,x} & B^{m2}_{xy\,x} & B^{f2}_{xx\,x} & B^{f2}_{yy\,x} & B^{f2}_{xy\,x} \\ B^{m2}_{xx\,y} & B^{m2}_{yy\,y} & B^{m2}_{xy\,y} & B^{f2}_{xx\,y} & B^{f2}_{yy\,y} & B^{f2}_{xy\,y} \end{pmatrix} \cdot \begin{pmatrix} \epsilon_{xx} \\ \epsilon_{yy} \\ \epsilon_{xy} \\ \kappa_{xx} \\ \kappa_{yy} \\ \kappa_{xy} \end{pmatrix} - \begin{pmatrix} C^{11}_{xx} & C^{11}_{xx} & C^{11}_{xx} & C^{11}_{xx} \\ & C^{11}_{xx} & C^{11}_{xx} & C^{11}_{xx} \\ & & C^{11}_{xx} & C^{11}_{xx} \\ & & & C^{11}_{xx} \end{pmatrix} \cdot \begin{pmatrix} E^{\eta 1}_{x} \\ E^{\eta 1}_{y} \\ E^{\eta 2}_{x} \\ E^{\eta 2}_{y} \end{pmatrix} \tag{3.2-16}$$

Now, we cuts to define the dissipative behaviour local At the macroscopic scale from behaviours within the RVE. Standard Generalised material theoretical framework (Halphen & Nguyen, 1975) is adopted fast to pseudo-potentials of dissipation At the microscopic scale, in order to take advantage of properties from Convex Analysis. Following the work by (Suquet, 1987), we get the macroscopic pseudo-potentials of dissipation depending one the disastrous of variable D^{ζ} , $\mathbf{E}^{\eta\zeta}$, by the same average principle ace gives for the free energy density.

Hyp.11: For the sake of simplicity, dissipative phenomena considered At the microscopic scale, within the RVE, are defined with the following threshold functions for concrete ramming and steel-concrete debonding (assuming constant threshold parameters k_0 and σ_{crit} , without hardening…), and the associated normality rules. We assumes that threshold positive parameter σ_{crit} is the same for all steel rebar in the RVE, whatever the bar diameter (it could Be easily enhanced). Then, threshold functions read:

$$f_{d^{\zeta}}(g^{\zeta}) = g^{\zeta} - k_0 \leq 0 \quad \text{and} \quad f^{\alpha}_{\eta\zeta}(\sigma^{\zeta}_{\alpha n}) = (\sigma^{\zeta}_{\alpha n})^2 - \sigma^2_{crit} \leq 0 \tag{3.2-17}$$

where $g^{\zeta} = -\frac{\partial w^{c}}{\partial d^{c}}$ is the microscopic energy concrete restitution disastrous for damaged in domain Ω_{sd}^{ζ} *and* Ω_{dm}^{ζ} and $\sigma_{\alpha n}^{\zeta}$ are the tangential components of microscopic stress vector $\boldsymbol{\sigma}.\mathbf{n}$ At the Γ_{b}^{ζ} interface. Thesis threshold functions define convex reversibility domains.

Remark 6:

> *The microscopic ramming threshold function results from the chosen ramming model quoted in Hyp 2 and not explicitly defined until now. The sliding threshold function results from Hyp 3 and Hyp 4.*

By means of the Legendre-Fenchel' S transform applied one the indicatrix functions of previously defined reversibility domains, we get the following pseudo-potentials of dissipation:

$$\varphi_{d}^{*}\left(\dot{d}^{\zeta}\right) = k_{0}|\dot{d}^{\zeta}| \quad \text{and} \quad \varphi_{\alpha}^{*\eta\zeta}\left(\dot{\eta}_{\alpha}^{\zeta}\right) = \sigma_{crit}.|\dot{\eta}_{\alpha}^{\zeta}(x_{\alpha})| \tag{3.2-18}$$

Thesis pseudo-potentials are convex, positively homogeneous of dismantles one, ensuring the positivity of variable dissipation for any acceptable disastrous of ramming internal $\dot{d}^{\zeta}$ and sliding ones $\dot{\eta}_{\alpha}^{\zeta}(x_{\alpha})$ (Hyp 10) At steel-concrete interfaces Γ_{b}^{ζ} , according to the Clausius-Duhem' S inequality;

Associated flow rules corresponding to the sub-gradients of threshold functions (*3.2-17*) give the disastrous of ramming variables in Ω_{dm}^{ζ} and sliding variable At Γ_{b}^{ζ} :

$$\dot{d}^{\zeta} = \dot{\lambda}_{d^{\zeta}} \frac{\partial f_{d^{\zeta}}\left(g^{\zeta}\right)}{\partial g^{\zeta}} = \dot{\lambda}_{d^{\zeta}} \quad \text{and} \quad \left[\!\left[\dot{u}_{\alpha}^{\zeta}\right]\!\right] = \dot{\eta}_{\alpha}^{\zeta} = \dot{\lambda}_{\eta^{\zeta}}^{\alpha} \frac{\partial f_{\eta^{\zeta}}^{\alpha}(\sigma_{\alpha 3}^{\zeta})}{\partial \sigma_{\alpha n}^{\zeta}} = 2\,\sigma_{\alpha n}^{\zeta} \dot{\lambda}_{\eta^{\zeta}}^{\alpha} \tag{3.2-19}$$

where $\dot{\lambda}_{d^{\zeta}}$ and $\dot{\lambda}_{\eta^{\zeta}}^{\alpha}$ are all positive scalars determined through the consistency condition: $\dot{f}_{d^{\zeta}} = 0$ and $\dot{f}_{\eta^{\zeta}}^{\alpha} = 0$. Therefore:

$$\dot{d}^{\zeta} = 2\frac{\left(-\boldsymbol{\varepsilon}:\mathbf{a}^{k'}\left(d^{\zeta}\right):\dot{\boldsymbol{\varepsilon}}\right)_{+}}{\boldsymbol{\varepsilon}:\mathbf{a}^{k''}\left(d^{\zeta}\right):\boldsymbol{\varepsilon}} \geq 0 \quad \text{and} \quad \left[\!\left[\dot{u}_{\alpha}^{\zeta}\right]\!\right] = \dot{\eta}_{\alpha}^{\zeta} = 2\,\sigma_{\alpha n}^{\zeta} \dot{\lambda}_{\eta^{\zeta}}^{\alpha} \geq 0 \tag{3.2-20}$$

Now, we fast edge dissipation pseudo-potential functions associated to macroscopic criteria (yield surfaces), being not-negative in actual evolutions and assumed to Be positively homogeneous of dismantles one in terms of the missed variable internal, and the internal variable flow rules. According to the work of (Suquet, 1987) and inspired from (Stolz, 2010), the macroscopic mechanical intrinsic dissipation edge Be defined ace follows:

$$\begin{aligned} D\left(\dot{\mathbf{D}}, \dot{\mathbf{E}}^{\eta}\right) &= \left\langle\left\langle \boldsymbol{\sigma}:\dot{\boldsymbol{\varepsilon}}\right\rangle\right\rangle_{\Omega} - \frac{H}{|\Omega|}\int_{\Gamma_{b}^{\zeta}} w_{,\boldsymbol{\varepsilon}}:\boldsymbol{\varepsilon}_{,\eta^{\zeta}}.\,\dot{\boldsymbol{\eta}}^{\zeta}\,dS - \left\langle\left\langle \dot{w}\left(\boldsymbol{\varepsilon}, d^{\rho}\right)\right\rangle\right\rangle_{\Omega} \\ &= G^{\rho}\dot{D}^{\rho} + \boldsymbol{\Sigma}^{\eta\zeta}.\dot{\mathbf{E}}^{\eta\zeta} \end{aligned} \tag{3.2-21}$$

Where $w\left(\boldsymbol{\varepsilon}, d^{\rho}\right)$ is the free energy density of each material composing the RVE; let custom note that $w_{,\varepsilon} : \varepsilon_{,\eta^{\zeta}}$ designates the stress vector At the concrete-steel interface.

Remark 7:

Ounce again, this has generalization, dedicated to punt structure model, of the one-dimensional formulation proposed by (Combescure and al., 2013).

According to (Suquet, 1987), we define the macroscopic pseudo-potentials of dissipation associated to ramming and jump-sliding by the average one the RVE of to their microscopic corresponding expressions (*3.2-18*), and accounting for Hyp 10:

$$\begin{aligned}\Phi_d^*\left(\dot{D}^{\zeta}\right) &= \left\langle\left\langle \varphi_d^*\left(\dot{d}^{\zeta}\right)\right\rangle\right\rangle_{\Omega} = \frac{H}{|\Omega|}\int_{\Omega_{dm}^{\zeta}} k_0 |\dot{d}^{\zeta}|\, d\,\Omega \qquad = \frac{H\left|\Omega_{dm}^{\zeta}\right|}{|\Omega|} k_0 \left|\dot{D}^{\zeta}\right| \quad \text{and} \\ \Phi_{\alpha}^{*\eta\zeta}\left(\dot{E}_{\alpha}^{\eta\zeta}\right) &= \frac{H}{|\Omega|}\int_{\Gamma_b^{\zeta}} \varphi_{\alpha}^{*\eta\zeta}\left(\dot{\eta}_{\alpha}^{\zeta}\right) dS \qquad = \frac{H}{|\Omega|}\sigma_{crit}.|\dot{E}_{\alpha}^{\eta\zeta}|\int_{\Gamma_b^{\zeta}} \hat{\eta}_{\alpha}^{\zeta}(x_{\alpha})\, dS \\ &= \frac{H\left|\Gamma_b^{\zeta}\right|}{2|\Omega|}.\sigma_{crit}.|\dot{E}_{\alpha}^{\eta\zeta}|\end{aligned} \tag{3.2-22}$$

Thesis convex, positively homogeneous of dismantles one, macroscopic pseudo-potentials of dissipation are the Legendre-Fenchel' S conjugate functions of indicatrix functions of reversibility domains At the macroscopic scale. Macroscopic threshold functions edge then Be identified from the macroscopic mechanical intrinsic dissipation ace:

$$f_{d^{\zeta}}\left(G^{\rho}\right) = G^{\zeta} - G^{\zeta\, crit} \leq 0 \quad \text{and} \quad f_{\eta^{\zeta}}^{\alpha}\left(\Sigma_{\alpha}^{\eta\zeta}\right) = \left(\Sigma_{\alpha}^{\eta\zeta}\right)^2 - \left(\Sigma_{\alpha}^{\zeta\, crit}\right)^2 \leq 0 \tag{3.2-23}$$

where the macroscopic strengths are given by:

$$G^{\zeta\, crit} = \frac{H\left|\Omega_{dm}^{\zeta}\right|}{|\Omega|} k_0 \quad \text{and} \quad \Sigma_{\alpha}^{\zeta\, crit} = \frac{H\left|\Gamma_b^{\zeta}\right|}{2|\Omega|}\sigma_{crit} \tag{3.2-24}$$

Therefore, we get two ramming macroscopic strengths (upper and lower halves of the RVE) and oven jump sliding ones (one for each steel rebar). Finally, macroscopic flow rules take the forms of normality rules, since the standard generalised properties At microphone-scale are simply transferred to macro-scale the:

$$\dot{D}^{\rho} = \dot{\lambda}_{d^{\rho}} \frac{\partial f_{d^{\rho}}\left(G^{\rho}\right)}{\partial G^{\rho}} = \quad \dot{\lambda}_{d^{\rho}} \quad \text{and} \quad \dot{E}_{\alpha}^{\eta\zeta} = \dot{\lambda}_{\eta^{\zeta}}^{\alpha} \frac{\partial f_{\eta^{\zeta}}^{\alpha}\left(\Sigma_{\alpha}^{\eta\zeta}\right)}{\partial \Sigma_{\alpha}^{\eta\zeta}} = 2\,\Sigma_{\alpha}^{\eta\zeta}\,\dot{\lambda}_{\eta^{\zeta}}^{\alpha} \tag{3.2-25}$$

where $\dot{\lambda}_{(d^{\rho})}$ and $\dot{\lambda}_{\eta^{\zeta}}^{\alpha}$ are all positive scalars determined through the consistency conditions: $\dot{f}_{(d^{\rho})} = 0$ and $\dot{f}_{(\eta^{\zeta})}^{\alpha} = 0$.

Remark 8:

Macroscopic threshold functions and flow rules are similar to their microscopic homonyms modulo has scaling Factor. Indeed, dissipative phenomena At the microscopic scale are naturally similar to the one located At the macroscopic scale since the dissipative homogenization process boat create news sources (Suquet, 1987). According to the work of (Suquet, 1987), the considered microscopic internal ramming and sliding variable being uniform constant gold piecewise in the whole links concealment, one edge affirm, thanks to the arguments of convex analysis, that the standard generalised properties of materials, At the microscopic scale, are transferred to the macroscopic homogenised model. Hence, the formerly presented model with its free energy density and pseudo-potentials of dissipation edge Be classified ace has Standard Generalised model.

Remark 9:

Since microscopic and macroscopic threshold functions possible are similar, it is to choose enriched threshold functions for microscopic ramming and sliding. This new choice will then immediately Be translated At the macroscopic scale. However, the simple choice of very threshold functions, see Hyp 11, with one only threshold parameter restricts the number of parameters to identify. Therefore, it is expected that simple thesis threshold functions will Be sufficient for practical applications.

Remark 10:

According to Remark 5, ace tensor $\mathbf{B}$ *vanishes yew there is No ramming, then* $\mathbf{\Sigma}^{\eta\zeta}$ *vanishes too and the macroscopic jump sliding threshold boat Be reached before the macroscopic ramming one*.

4 Finite Element implementation

The non-linear DHRC constitutive model formulated for punt structural element has been implemented for has DKT-CST punt finite element family (Batoz, 1982), see [R3.07.03], allowing has rather efficient and changeable modelling of complex building geometries. We remark that the curvature tensor $\mathbf{K}$ has opposite components in the notations used by punts elements in *Code_Aster*, see [R3.07.03]: the sub-matrices $\mathbf{A}^{mf}$ and $\mathbf{B}^{f\zeta}$ cut to Be multiplied by -1 .

The numerical integration of DHRC constitutive model dregs one direct implicit time discretization method (Nguyen, 1977), (Simo & Taylor, 1985), which is included in the Newton' method with year elastic predictor step followed by has “plastic” corrector step, At the total balances equations internship.

At the beginning of each time step, trial generalised stress are calculated by assuming has fully elastic answer missed, with year elastic tensor evaluated for the previous damaged state. In what follows, the superscript $\{.\}^{+}$ associated to the unknown variable of the problem refers to the converged state local At the end of the integration, whereas the superscript $\{.\}^{-}$ refers to the previous converged state. Possible It is useful to differentiate activated and not activated macroscopic mechanisms among the six ones – two evolving ramming D^{ρ} variables, oven evolving debonding $\mathbf{E}^{\eta\rho}$ components – to avoid unnecessary computation. Therefore, At each Gauss not, we get back for initialising:

$$\begin{pmatrix} D^{\rho^{(1)}} \\ \mathbf{E}^{\eta\zeta^{(1)}} \end{pmatrix} = \begin{pmatrix} D^{\rho^{(-)}} \\ \mathbf{E}^{\eta\zeta^{(-)}} \end{pmatrix} \tag{4-1}$$

Then, the new internal variable are computed via has local implicit resolution of non-linear equations (flow rules) based one Newton' S method, At the k^{th} iteration:

$$\begin{pmatrix} D^{\rho^{(k+1)}} \\ \mathbf{E}^{\eta\zeta^{(k+1)}} \end{pmatrix} = \begin{pmatrix} D^{\rho^{(k)}} \\ \mathbf{E}^{\eta\zeta^{(k)}} \end{pmatrix} - \left(\mathbf{J}\right)^{(k)} . \begin{pmatrix} f_{d^\rho}\left(G^{\rho^{(k)}}\right) \\ f^{\alpha}_{\eta^\zeta}\left(\Sigma^{\eta\zeta^{(k)}}_{\alpha}\right) \end{pmatrix} \tag{4-2}$$

The Jacobian matrix $\mathbf{J}$ of all activated macroscopic threshold functions (*3.2-23*) is computed by means of the closed-form expression established hereafter yew all six thresholds are activated:

$$\mathbf{J}_{6\times 6} = \begin{pmatrix} \dfrac{-1}{G^{crit}}\left(\dfrac{\partial^2 W}{\partial D^\rho \partial D^\zeta}\right) & \dfrac{-1}{G^{crit}}\left(\dfrac{\partial \mathbf{B}^\zeta(\mathbf{D})}{\partial D^\zeta} : \begin{pmatrix}\mathbf{E}\\ \mathbf{K}\end{pmatrix} + \dfrac{\partial \mathbf{C}}{\partial D^\zeta}\mathbf{E}^{\eta\zeta}\right) \\ \dfrac{-2\boldsymbol{\Sigma}^\eta}{\left(\Sigma^{crit}\right)^2}\left(\dfrac{\partial \mathbf{B}^\zeta(\mathbf{D})}{\partial D^\zeta} : \begin{pmatrix}\mathbf{E}\\ \mathbf{K}\end{pmatrix} + \dfrac{\partial \mathbf{C}}{\partial D^\zeta}\mathbf{E}^{\eta\zeta}\right) & \dfrac{-2}{\left(\Sigma^{crit}\right)^2}\left(\mathbf{C}(\mathbf{D}).\boldsymbol{\Sigma}^\eta\right) \end{pmatrix} \tag{4-3}$$

We recall, see (*3.2-2*), that:

$$2\frac{\partial^2 W}{\partial D^\rho \partial D^\zeta} = \begin{pmatrix}\mathbf{E}\\ \mathbf{K}\end{pmatrix} : \frac{\partial^2 \mathbf{A}(\mathbf{D})}{\partial D^\rho \partial D^\zeta} : \begin{pmatrix}\mathbf{E}\\ \mathbf{K}\end{pmatrix} + 2\begin{pmatrix}\mathbf{E}\\ \mathbf{K}\end{pmatrix} : \frac{\partial^2 \mathbf{B}(\mathbf{D})}{\partial D^\rho \partial D^\zeta}.\mathbf{E}^\eta + \mathbf{E}^\eta . \frac{\partial^2 \mathbf{C}(\mathbf{D})}{\partial D^\rho \partial D^\zeta}.\mathbf{E}^\eta \tag{4-4}$$

Diagonal This matrix is, by construction of the tensors $\mathbf{A}(\mathbf{D})$, $\mathbf{B}(\mathbf{D})$, $\mathbf{C}(\mathbf{D})$.

The estimated new state is so corrected to satisfy the discretised forms of the thresholds of ramming and debonding, until has prescribed tolerance is reached one each threshold. The overview of the implicit integration algorithm is drawn At Figure 4-a. in has first step, the activated thresholds are determined. Then the disastrous of the corresponding internal variable are solved by the Newton' S method. The all six thresholds are verified, and yew summons other ones are reached, the non-linear system is updated. At the end, all the local variables are updated.

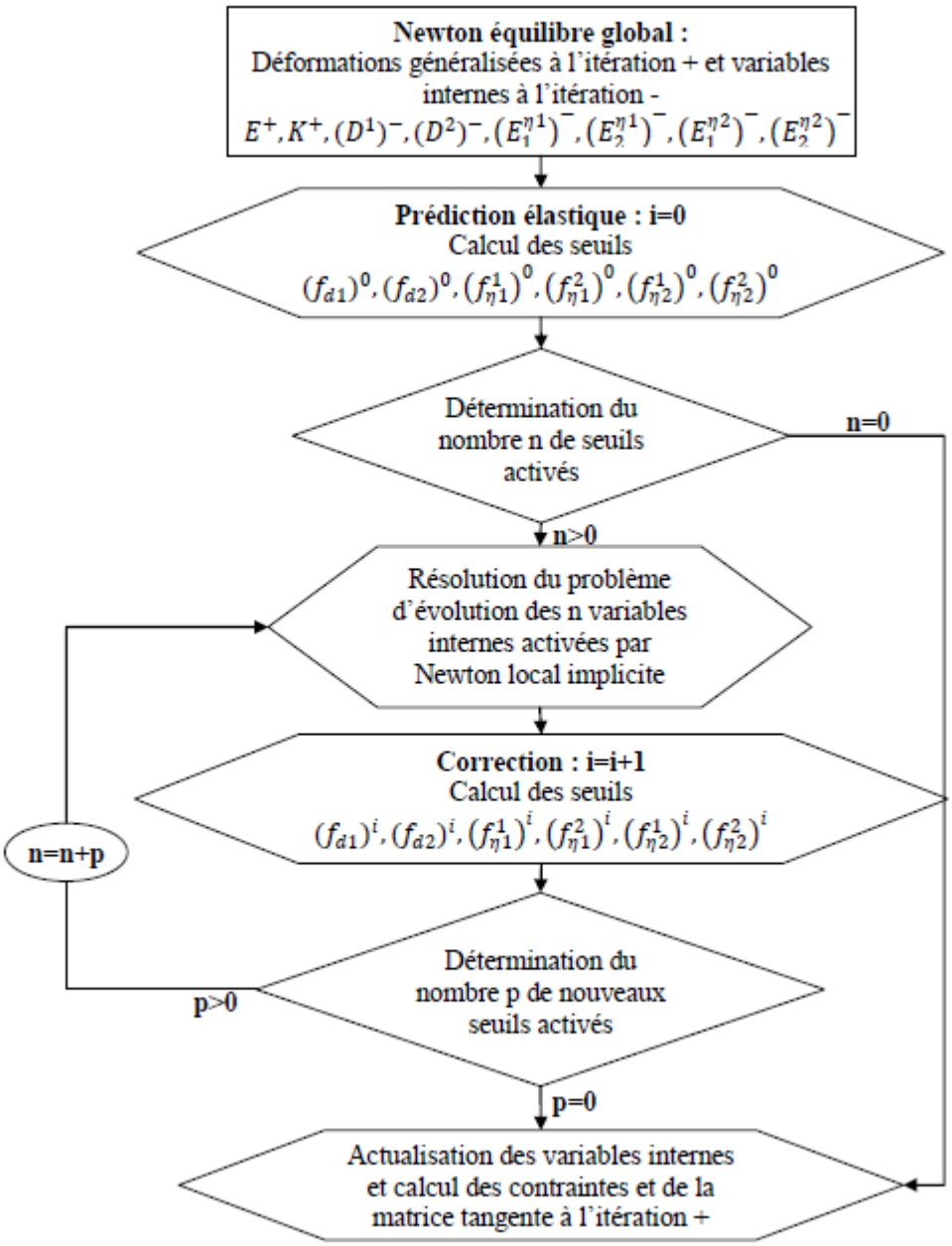

Figure 4-a : Constitutive Chart of the law implicit integration.

Ounce the calculation of the new internal variable is gives, we perform the new resulting stresses, see (3.2-11) and (3.2-12); finally one calculates the tangent stiffness operator from the first variations of $\mathbf{E}$ and $\mathbf{K}$ and corresponding first variations of $\mathbf{D}$ and $\mathbf{E}^{\eta\zeta}$:

$$\begin{pmatrix} \frac{d\mathbf{N}}{d\mathbf{E}} & \frac{d\mathbf{N}}{d\mathbf{K}} \\ \frac{d\mathbf{M}}{d\mathbf{E}} & \frac{d\mathbf{M}}{d\mathbf{K}} \end{pmatrix} = \begin{pmatrix} \mathbf{A}^{mm}(\mathbf{D}) & \mathbf{A}^{mf}(\mathbf{D}) \\ \mathbf{A}^{fm}(\mathbf{D}) & \mathbf{A}^{ff}(\mathbf{D}) \end{pmatrix} + \begin{pmatrix} \mathbf{A}^{mm}_{,\mathbf{D}}(\mathbf{D}).\mathbf{E} + \mathbf{A}^{mf}_{,\mathbf{D}}(\mathbf{D}).\mathbf{K} \\ \mathbf{A}^{fm}_{,\mathbf{D}}(\mathbf{D}).\mathbf{E} + \mathbf{A}^{ff}_{,\mathbf{D}}(\mathbf{D}).\mathbf{K} \end{pmatrix} \otimes \begin{pmatrix} \frac{\partial \mathbf{D}}{\partial \mathbf{E}} \\ \frac{\partial \mathbf{D}}{\partial \mathbf{K}} \end{pmatrix}$$
$$+ \begin{pmatrix} \mathbf{B}^{m\zeta}_{,\mathbf{D}}(\mathbf{D}).\mathbf{E}^{\eta\zeta} \\ \mathbf{B}^{f\zeta}_{,\mathbf{D}}(\mathbf{D}).\mathbf{E}^{\eta\zeta} \end{pmatrix} \otimes \begin{pmatrix} \frac{\partial \mathbf{D}}{\partial \mathbf{E}} \\ \frac{\partial \mathbf{D}}{\partial \mathbf{K}} \end{pmatrix} + \begin{pmatrix} \mathbf{B}^{m\zeta}(\mathbf{D}) \\ \mathbf{B}^{f\zeta}(\mathbf{D}) \end{pmatrix} \otimes \begin{pmatrix} \frac{\partial \mathbf{E}^{\eta\zeta}}{\partial \mathbf{E}} \\ \frac{\partial \mathbf{E}^{\eta\zeta}}{\partial \mathbf{K}} \end{pmatrix} \quad (4\text{-}5)$$

Opposite The last vectors are obtained from of the Jacobian matrix $\mathbf{J}$ of all macroscopic threshold functions, taking advantage of consistency equations $\dot{f}_{(d^\rho)}=0$ and $\dot{f}^{\alpha}_{(\eta^\zeta)}=0$, see equations (3.2-25) and (4-3), where superscript τ means m however f according the box:

$$\begin{pmatrix} \frac{\partial \mathbf{D}}{\partial \mathbf{E}} & \frac{\partial \mathbf{D}}{\partial \mathbf{K}} \\ \frac{\partial \mathbf{E}^{\eta\zeta}}{\partial \mathbf{E}} & \frac{\partial \mathbf{E}^{\eta\zeta}}{\partial \mathbf{K}} \end{pmatrix} = \mathbf{J}^{-1}.\begin{pmatrix} \mathbf{A}^{m\tau}_{,\mathbf{D}}(\mathbf{D}).\begin{pmatrix} \mathbf{E} \\ \mathbf{K} \end{pmatrix} + \mathbf{B}^{m\zeta}_{,\mathbf{D}}(\mathbf{D}).\mathbf{E}^{\eta\zeta} & \mathbf{A}^{f\tau}_{,\mathbf{D}}(\mathbf{D}).\begin{pmatrix} \mathbf{E} \\ \mathbf{K} \end{pmatrix} + \mathbf{B}^{f\zeta}_{,\mathbf{D}}(\mathbf{D}).\mathbf{E}^{\eta\zeta} \\ 2.\boldsymbol{\Sigma}^{\eta}.\mathbf{B}^{m}(\mathbf{D}) & 2.\boldsymbol{\Sigma}^{\eta}.\mathbf{B}^{f}(\mathbf{D}) \end{pmatrix} \quad (4\text{-}6)$$

4.1 Parameter identification procedure

Present We in this section the general approach out carried in order to identify DHRC parameters. The needed microscopic scale dated: geometry and material characteristics, and the hand steps of the proposed automated procedure are detailed.

4.2 Identification approach

The hand difficulty to Be overcome hereafter is to ensure that with has limited number of auxiliary problems solutions, we will Be whitebait to identify DHRC parameters that:

- cover the space of macroscopic states ($\mathbf{E}$, $\mathbf{K}$, D^ζ , $\mathbf{E}^{\eta\zeta}$),
- cut has generic dependency one macroscopic variable ramming D^ζ , from the sound state, distinguishing tensile and compressive modes,
- ensure continuity of resulting stresses ($\mathbf{N}$, $\mathbf{M}$, $\boldsymbol{\Sigma}^{\eta\zeta}$) At each mode changes,
- ensure the convexity of the macroscopic free energy density.

We decided to perform nap “snapshots” of microscopic states for has limited number of selected macroscopic ones, and to entrust the task of determining the parameters dependency to D^ζ to has least public gardens method and year appropriate selected function of D^ζ . We recall from (Combescure and al., 2013), that in one dimension, yew the microscopic ramming function, controlling the elastic stiffness degradation $\mathbf{a}^c(d)$, is expressed ace $\xi(d)=(\alpha+\gamma d)/(\alpha+d)$ (which is decreasing convex for $\gamma\leq 1$) then the macroscopic one-dimensional elastic tensor $\mathbf{A}$ follows the same dependency and is equal to $\mathbf{A}=\mathbf{A}^0(\alpha_A+\gamma_A D)/(\alpha_A+D)$, with $\gamma_A\leq 1$, similarly for the other tensors $\mathbf{B}$ and $\mathbf{C}$. This ensures the convexity of the resulting Helmholtz free energy function, provided that γ is not “excessively” negative.

Ace shown in the previous section, from the solutions of has set of auxiliary elastic problems, we cuts to identify the components of three tensors $\mathbf{A}$, $\mathbf{B}$ and $\mathbf{C}$ with to their macroscopic variable ramming D^ζ dependency. Two macroscopic threshold been worth for ramming and sliding need also to Be determined.

Hyp.12. According to the results obtained for the macroscopic one-dimensional box (Combescure and al., 2013), we assumes the generic following dependency one D^ζ variable of the macroscopic tensors components (the particular expression for tensor $\mathbf{B}$ resulting from Remark 6):

$$\frac{\alpha+\gamma D^\zeta}{\alpha+D^\zeta} \quad \text{for tensors } \mathbf{A} \text{ and } \mathbf{C}; \quad \frac{\gamma D^\zeta}{\alpha+D^\zeta} \quad \text{for coupling tensor } \mathbf{B} \tag{4.2-1}$$

Of chases this compromised will cuts to Be assessed by comparison of DHRC model results with available experimental dated one actual RC structures and usual loading paths.

4.3 Microscopic material parameters in RVE Ω

According to assumptions Hyp 1, steel is considered ace linear elastic (defined by its Young' S modulus E_s and Poisson' S ratio ν_s). Hyp 2 assume that concrete is elastic and damageable. The to lath is defined by the following constitutive model $\boldsymbol{\sigma}=\mathbf{a}^c(d):\boldsymbol{\varepsilon}$, d being the microscopic scalar variable ramming. In particular, we cuts to define ramming dependency of elastic constant, how to tensile deal with and compressive modes, the relationship with usual concrete behaviour parameters, induced anisotropy and the distribution of damaged sub-domains into the RVE according to macroscopic states

Hyp. 13. Concrete Microscopic elasticity tensor $\mathbf{a}^c(d)$ is defined by its initial sound isotropic elastic tensor $\mathbf{a}^c(0)$, characterised by Young' S modulus E_c and Poisson' S ratio ν_c . For $d>0$, the elasticity tensor components are reduced by has multiplicative decreasing convex ramming function $\xi(d)$. We proposes the generic mathematical expression $\xi(d)=(\alpha+\gamma d)/(\alpha+d)$, with $\gamma<1$ – ensuring has stiffness degradation for increasing ramming d – which produces has bilinear uniaxial strain-stress answer for monotonic loading paths, see section §4.1 of (Combescure and al., 2013).

Hyp. 14. In order to distinguish between tensile and compressive states in concrete sub-domains we introduce has dissymmetry in $\xi(d)$. To this end, the microscopic ramming function is modified through the uses of has Heaviside' S function $H(x)$ and then takes the following forms:

$$\xi(d,x)=\frac{\alpha_+ +\gamma_+ d}{\alpha_+ +d}H(x)+\frac{\alpha_- +\gamma_- d}{\alpha_- +d}H(-x) \tag{4.3-1}$$

This means that ramming function ξ includes oven parameters:

$$\begin{cases} \alpha_+>0,\ \gamma_+\le 1, & \text{for tension behaviour} \\ \alpha_->0,\ \gamma_-\le 1, & \text{for compression behaviour} \end{cases} \tag{4.3-2}$$

In practice, we take $\alpha_+=1$ without getting out any generality, ace the only consequence is to standardizes the variable ramming d . In five addition, we will take the following set of been worth of d : $\{0.,0.5,2.,10.,20.\}$, considered to cover has sufficient arranges of ramming for year accurate identification. This relative choice seems to Be the better compromised between error and computing burden.

Concrete free energy density being $w(\varepsilon,d)=\frac{1}{2}\boldsymbol{\varepsilon}:\mathbf{a}^c(d):\boldsymbol{\varepsilon}$, we define energy release disastrous by $g(\varepsilon,d)=-w_{,d}(\varepsilon,d)$, and convex reversibility domain by the constant ramming criterion with the threshold been worth k_0 , see Hyp 11 and expression (3.2-17):

$$g(\varepsilon, d) = -\frac{1}{2}\boldsymbol{\varepsilon} : \mathbf{a}^{c}_{,d}(d) : \boldsymbol{\varepsilon} \quad \leq k_0 \tag{4.3-3}$$

According to uniaxial stress-strain curves of concrete (CEB-FIP Model Codes 1990.1993), we uses the usual following parameters: concrete tensile f_t and compression f_c strength been worth (to form being associated to has fracture energy G_f , the later to has compression strain ε_{cm}) and we assumes has threshold been worth f_{dc} of initial ramming in compression. So, assuming has multilinear regression of the experimental stress-strain curve through this concrete constitutive model, we edge associate the been worth of α_- , γ_- , γ_+ and k_0 with usual engineering parameters f_t , G_f , f_c , ε_{cm} , f_{dc} .

Let custom consider has pure tensile uniaxial membrane stress loading box N^t_{11} , in the x_1 direction, one has sound RVE, i.e with zero-valued internal variable: indeed the problem remains linear. Thus, referring to equations (3.2-14) and (3.2-24), we may fast the macroscopic energy restitution missed, which is quadratic in N^t_{11} :

$$G^{\zeta} = -\frac{1}{2}\left(\mathbf{A}^{-1}(\mathbf{0}).N_{11}\right) : \mathbf{A}_{,D^{\zeta}}(\mathbf{0}) : \left(\mathbf{A}^{-1}(\mathbf{0}).N_{11}\right) \quad = \hat{G}^{t\zeta}_{N_{11}}.\left(N^t_{11}\right)^2 \tag{4.3-4}$$

In parallel, we calculate the microscopic energy restitution disastrous (4.3-3), using (3.1-1) to fast the local strain tensor $\boldsymbol{\varepsilon}$ using the generalised strain measures $\mathbf{E}$, $\mathbf{K}$ obtained by inverting (3.2-11) and (3.2-12) to fast them from N^t_{11} :

$$g = -\frac{1}{2}\boldsymbol{\varepsilon} : \mathbf{a}^{c}_{,d}(0) : \boldsymbol{\varepsilon} \quad = \hat{g}^{t}_{N_{11}}.\left(N^t_{11}\right)^2 \tag{4.3-5}$$

Moreover, we calculate the stress tensor $\boldsymbol{\sigma} = \mathbf{a}^{c}(0) : \boldsymbol{\varepsilon}$ field At any not within concrete the RVE domain Ω^{ζ}_{c} , and we given the maximum been worth $\hat{\sigma}^{max}_{t}.|N^t_{11}|$ of the eigen-been worth of this tensor, according to has Rankine criterion. Equating with the given f_t parameter, we get the critical been worth $\tilde{N}^t_{11}$ in tension, then the following relation, see also (3.2-24):

$$\left(\tilde{N}^t_{11}\right)^2 = \left(\frac{f_t}{\hat{\sigma}^{max}_{t}}\right)^2 = \frac{k_0}{\hat{g}^{t}_{N_{11}}} \quad = \quad \frac{G^{\zeta crit}}{\hat{G}^{t\zeta}_{N_{11}}} = \frac{k_0}{\hat{G}^{t\zeta}_{N_{11}}}\frac{H\left|\Omega^{\zeta}_{dm}\right|}{|\Omega|} \tag{4.3-6}$$

Therefore, we edge deduce the been worth of k_0 from f_t , $\hat{g}^{t}_{N_{xx}}$ and $\hat{\sigma}^{max}_{t}$. Of chases, the local quantities $\hat{\sigma}^{max}_{t}$ and $\hat{g}^{t}_{N_{11}}$ are depending one α_- , γ_- , γ_+ been worth, while the two been worth $\hat{G}^{t\zeta}_{N_{11}}$ (for $\zeta = 1$ and $\zeta = 2$) one depends the macroscopic $\mathbf{A}(\mathbf{0})$ tensor components and all the α^A and γ^A parameters to fast the derivative $\mathbf{A}_{,D^{\zeta}}(\mathbf{0})$.

We could easily proceed in the same manner for has pure compressive uniaxial membrane stress loading box N^c_{11} . Nevertheless, we assumes that it is satisfactory to follow the expression shown in section §4.2 of (Combescure, Dumontet, & Voldoire, 2013), which correspond to has pure one-dimensional box:

$$\frac{f_t^2(1-\gamma_+)}{\alpha_+} = \frac{f_{dc}^2(1-\gamma_-)}{\alpha_-} \tag{4.3-7}$$

(One recalls that $\alpha_+=1$). We proposes to roughly approximate the post-elastic share of the concrete uniaxial compression curve by has linear ranging segment from the first ramming threshold f_{dc} to the extremum (ε_{cm} , f_c), so that γ_- belonging to $]0.,1.]$. Then:

$$\gamma_-=\frac{\left|f_c-f_{dc}\right|}{\left|E_c\varepsilon_{cm}-f_{dc}\right|} \tag{4.3-8}$$

Hyp. 15. Finally, we proposes to choose γ_+ so that the softening post-peak tensile path becomes sufficiently weak in order to avoid any softening of the homogenised answer by the DHRC constitutive model. It is expected that provided that γ_+ remains closed to zero, even negative, the homogenised free energy density will Be strictly convex (this will Be checked At the end of the identification process, see also section 7.2). So, we don' T make uses of G_f .

Hence, from (4.3-7), we get:

$$\alpha_-=\frac{f_{dc}^2\left(1-\gamma_-\right)}{f_t^2\left(1-\gamma_+\right)} \tag{4.3-9}$$

Remark 11:

The series expansions At order 2 of the $\xi(d)$ function are:

$$\xi(d)=1+\frac{\gamma-1}{\alpha}d+o(d^2)=\gamma+\frac{1-\gamma}{d}\alpha+o(\alpha^2)$$
$$=1+d(\gamma-1)(2-\alpha)+o(d^2)+o((\alpha-1)^2)$$

Therefore, in the vicinity of $d=0$, $\frac{\gamma-1}{\alpha}$ controls the negative slope of $\xi(d)$; so, this slope is directly inversely proportional to α : it has to Be kept in mind to choose the α_- parameter been worth; a priori, we edge expect that $\alpha_->1$. Broad For ramming been worth, $\xi(d)$ tighten to the asymptotic been worth γ_- . Finally, around $\alpha_-=1$ been worth, the negative slope of $\xi(d)$ is γ_--1 .

Hyp. 16. Given the orthotropic geometry of the punt, we assumes that ramming induces orthorhombic behaviour, and define the nine orthorhombic elastic constant from the been worth of sound concrete Lamé' S constant λ_c , μ_c . Principal The material directions in the (x_1,x_2) plane are chosen according to the macroscopic membrane strain directions, respectively: At $0°$ for the box of dilation strains gold jump sliding, At $45°$ for the box of shear strains only.

Even yew this choice could appear ace arbitrary, and edge Be replaced by another one, it is believed that it will Be satisfactory for our purposes

Hyp. 17. Variable x in equation (4.3-1) is chosen to Be macroscopic membrane strain component $E_{\alpha\beta}$ for the diagonal terms of tensors $\mathbf{A}$, $\mathbf{B}$ and $\mathbf{C}$ and tensor invariant $\mathrm{tr}\,\mathbf{E}$ for to their off-diagonal terms. Therefore we are neglecting the microscopic correctors influence in the damaged elastic tensor microscopic been worth. Moreover, this choice keeps the needed symmetry properties of homogenised tensors $\mathbf{A}$, $\mathbf{B}$ and $\mathbf{C}$. For bending auxiliary problems, we replaces tensor $\mathbf{E}$ by tensor $\mathbf{K}$. For jump sliding auxiliary problems ($E_{\alpha\beta}=0$, $K_{\alpha\beta}=0$, see equation (3.1-5) tensile ramming is expected in the considered concrete sub-domain of the RVE, thus parameter γ_+ is used. Consequently, we set:

$$\lambda_+(d)=\lambda_c\frac{\alpha_++\gamma_+d}{\alpha_++d}\quad;\quad\lambda_-(d)=\lambda_c\frac{\alpha_-+\gamma_-d}{\alpha_-+d}\quad;\quad\mu_+(d)=\mu_c\frac{\alpha_++\gamma_+d}{\alpha_++d}\quad;\quad\mu_-(d)=\mu_c\frac{\alpha_-+\gamma_-d}{\alpha_-+d}\qquad(4.3\text{-}10)$$

For jump sliding auxiliary problems, the orthorhombic elastic constant are:

$$E_1=E_2=\mu_+\frac{3\lambda_++2\mu_+}{\lambda_++\mu_+}\quad;\quad E_3=\mu_-\frac{3\lambda_++2\mu_-}{\lambda_++\mu_-}\quad;$$
$$G_{12}=\mu_+\quad;\quad G_{23}=G_{31}=\mu_-\quad;\quad v_{12}=v_{23}=v_{31}=\frac{\lambda_+}{2(\lambda_++\mu_-)}\qquad(4.3\text{-}11)$$

For macroscopic membrane and bending links auxiliary problems (3.1-5), they fulfil:

Yew $E_{11}+E_{22}+E_{12}>0$ however $K_{11}+K_{22}+K_{12}>0$ then we set

$$G_{12}=\mu_+\quad;\quad\tilde{\lambda}=\lambda_+\quad;\quad E_1=\mu_+\frac{3\tilde{\lambda}+2\mu_+}{\tilde{\lambda}+\mu_+}\quad;\quad E_2=\mu_+\frac{3\tilde{\lambda}+2\mu_+}{\tilde{\lambda}+\mu_+}$$

else

$$G_{12}=\mu_-\quad;\quad\tilde{\lambda}=\lambda_-\quad;\quad E_1=\mu_-\frac{3\tilde{\lambda}+2\mu_-}{\tilde{\lambda}+\mu_-}\quad;\quad E_2=\mu_-\frac{3\tilde{\lambda}+2\mu_-}{\tilde{\lambda}+\mu_-}\quad.\qquad(4.3\text{-}12)$$

Then $E_3=\mu_-\frac{3\tilde{\lambda}+2\mu_-}{\tilde{\lambda}+\mu_-}\quad;\quad G_{23}=G_{31}=\mu_-\quad;\quad v_{12}=v_{23}=v_{31}=\frac{\lambda_+}{2(\tilde{\lambda}+\mu_-)}$

Remark 12:

Therefore, in pure shear strain box, compressive elastic constant $\tilde{\lambda}=\lambda_-$ is assigned.

Hyp. 18. Finally, we assumes several distributions of concrete sub-domains within the RVE, according to the needed dissymmetry of ramming distribution (Hyp 7, Hyp 8, Hyp 10). Hence we will consider the following three kinds of distributions of Ω_i^ζ sub-domains ($i=sd,dm$) for sound gold damaged concrete in upper gold lower halves of the RVE ($\zeta=1,2$), with previous isotropic elastic constant in the sound concrete Ω_{sd}^ζ sub-domains and orthotropic elastic constant (for five ramming been worth taken in the set: $\{0.,0.5,2.,10.,20.\}$; we performed has sensitivity analysis whose conclusion showed that it has good compromised) and principal material directions in the damaged Ω_{dm}^ζ sub-domains. Thesis distributions constitute three kinds of RVE, named hereafter Ω_X , see Figure 2 3, and Ω_Y (first principal material direction At $0°$ in the (x_1 , x_2) plane), $\Omega_{(45°)}$ (first principal material direction At $45°$ in the (x_1 , x_2) plane), see Table 4 1.

Thesis three kinds respective of RVE are designed to deal with the directions of macroscopic loading. The $\Omega_{(45°)}$ RVE is used for the shear strains loading boxes, where No separation in the (x_1 , x_2) plane is needed. So, in those boxes the contribution of jump sliding vanishes, ace we edge deduce from the corresponding auxiliary problems. Conversely, ace we need to perform given cross-country race products between corrector fields to the off-diagonal components of the homogenised tensors $\mathbf{A}$, $\mathbf{B}$, $\mathbf{C}$, we cuts to out curry calculations one the three kinds of RVEs for membrane and bending macroscopic strains.

Table 4 1. Ω_i^ζ subdomains assignments according to each kind of RVE.

RVE	loading	damaged half	Ω_i^ζ sub-domains
Ω_X	membrane, bending and jump sliding	$d^1 \geq 0$, $d^2 = 0$	for $x_3 > 0$: Ω_{dm}^1 for $x_1 > 0$ and for $x_1 < 0$ for $x_3 < 0$: Ω_{sd}^2
Ω_X	membrane, bending and jump sliding	$d^1 = 0$, $d^2 \geq 0$	for $x_3 > 0$: Ω_{sd}^1 for $x_3 < 0$: Ω_{dm}^2 for $x_1 > 0$ and for $x_1 < 0$
Ω_Y	membrane, bending and jump sliding	$d^1 \geq 0$, $d^2 = 0$	for $x_3 > 0$: Ω_{dm}^1 for $x_2 > 0$ and for $x_2 < 0$ for $x_3 < 0$: Ω_{sd}^2
Ω_Y	membrane, bending and jump sliding	$d^1 = 0$, $d^2 \geq 0$	for $x_3 > 0$: Ω_{sd}^1 for $x_3 < 0$: Ω_{dm}^2 for $x_2 > 0$ and for $x_2 < 0$
$\Omega_{(45°)}$	membrane and bending	$d^1 \geq 0$, $d^2 = 0$	for $x_3 > 0$: Ω_{dm}^1 for any x_1 , x_2 for $x_3 < 0$: Ω_{sd}^2
$\Omega_{(45°)}$	membrane and bending	$d^1 = 0$, $d^2 \geq 0$	for $x_3 > 0$: Ω_{sd}^1 for $x_3 < 0$: Ω_{dm}^2 for any x_1 , x_2

Remark 13:

> *Concrete note that the volume of damaged sub-domains is ¼ of total for both Ω_X , Ω_Y RVEs and ½ of total for $\Omega_{(45°)}$ RVE.*

Finally, we cuts to solve 207 auxiliary problems: nine ramming (d^1 , d^2) been worth combinations (with five d^ζ been worth taken in the set: {0,0.5, 2. , 10. , 20.}) times twenty-three kinds of RVE Ω_i^ζ sub-domains distributions and loading conditions: nine with the Ω_X RVE according to the x_1 direction (five without jump sliding, oven with sliding conditions), nine with the Ω_Y RVE according to the x_2 direction, five with the $\Omega_{(45°)}$ RVE with orthotropic reference frame rotated 45 ° (without jump sliding). The following Table 4 2 sums up thesis boxes; it is depending also for pure macroscopic bending loading boxes ($K_{\alpha\beta}$ instead of $E_{\alpha\beta}$), adding so fifteen times nine (135) other elastic problems to solve.

Table 4 2. Ω_i^ζ subdomains assignments according to each kind of RVE.

RVE Ω_X	RVE Ω_Y	RVE $\Omega_{(45°)}$
macroscopic membrane strain	macroscopic membrane strain	macroscopic membrane strain
$E_{11} = -1$, $E_{22} = 0$, $E_{12} = 0$ $E_{11} = 1$, $E_{22} = 0$, $E_{12} = 0$	$E_{11} = -1$, $E_{22} = 0$, $E_{12} = 0$ $E_{11} = 1$, $E_{22} = 0$, $E_{12} = 0$	$E_{11} = -1$, $E_{22} = 0$, $E_{12} = 0$ $E_{11} = 1$, $E_{22} = 0$, $E_{12} = 0$

$E_{11}=0$, $E_{22}=-1$, $E_{12}=0$ $E_{11}=0$, $E_{22}=1$, $E_{12}=0$ $E_{11}=0$, $E_{22}=0$, $E_{12}=0.5$	$E_{11}=0$, $E_{22}=-1$, $E_{12}=0$ $E_{11}=0$, $E_{22}=1$, $E_{12}=0$ $E_{11}=0$, $E_{22}=0$, $E_{12}=0.5$	$E_{11}=0$, $E_{22}=-1$, $E_{12}=0$ $E_{11}=0$, $E_{22}=1$, $E_{12}=0$ $E_{11}=0$, $E_{22}=0$, $E_{12}=0.5$
jump sliding	jump sliding	No jump sliding
$E_1^{\eta 1}=1$, other zero $E_2^{\eta 1}=1$, other zero $E_1^{\eta 2}=1$, other zero $E_2^{\eta 2}=1$, other zero	$E_1^{\eta 1}=1$, other zero $E_2^{\eta 1}=1$, other zero $E_1^{\eta 2}=1$, other zero $E_2^{\eta 2}=1$, other zero	_

4.4 Macroscopic material parameters to Be determined

After solving the 342 auxiliary problems, we cuts At our disposal enough information one the corrector fields $\boldsymbol{\chi}^{\alpha\beta}$ in membrane, $\boldsymbol{\xi}^{\alpha\beta}$ in bending and $\boldsymbol{\chi}^{\eta_\alpha^\rho}$ for jump sliding to compute the $\mathbf{A}$, $\mathbf{B}$, $\mathbf{C}$ macroscopic tensors components, see section 3.1.2. All components are expressed in the reference frame determined by the steel bar grids.

4.4.1 Tensor $\mathbf{A}$

Tensor $\mathbf{A}$ is the stiffness elastic damageable tensor of the homogenised RC punt tensor, see equations (3.2-4, - 5, - 6). It has symmetric fourth order tensor of the tangent planes (see Remark 3) comprising membrane, bending and coupling terms. Possible It is to blind it using Voigt' S notation for tensors components in the reference frame of steel rebar grids, by means of 3×3 matrices:

$$\mathbf{A}=\begin{bmatrix}\mathbf{A}^{mm} & \mathbf{A}^{mf}\\ \mathbf{A}^{fm} & \mathbf{A}^{ff}\end{bmatrix} \quad \text{where} \quad \mathbf{A}^{mf}=\mathbf{A}^{fm} \tag{4.4-1}$$

From equations (3.2-5), we deduce that $\mathbf{A}^{mm}$ and $\mathbf{A}^{ff}$ matrices are symmetric, whereas in general No symmetry argument hold for $\mathbf{A}^{mf}$ matrix. Therefore we cuts $21=6+6+9$ components to Be determined for tensor $\mathbf{A}$.

Remark 14:

Yew the RC punt present mirror symmetry (symmetry around the medium planes), then both membrane-bending coupling matrices $\mathbf{A}^{mf}$ and $\mathbf{A}^{fm}$ should vanish ace long ace ramming variables verify $D^1=D^2$.

Hyp. 19 . We define the parameters α^A and γ^A characterising the dependency one macroscopic variable ramming D^ζ (Hyp 12) and the tensile/compressive distinction in positive membrane but/negative curvature in bending of the tensor $\mathbf{A}$ components (Hyp 14) by:

$$A^{\tau\tau}_{\beta\delta\lambda\mu}(\mathbf{D},x)=\frac{1}{2}A^{0\,\tau\tau}_{\beta\delta\lambda\mu}\left(\frac{\alpha^{A\varsigma\tau\tau\,1}_{\beta\delta\lambda\mu}+\gamma^{A\varsigma\tau\tau\,1}_{\beta\delta\lambda\mu}D^1}{\alpha^{A\varsigma\tau\tau\,1}_{\beta\delta\lambda\mu}+D^1}+\frac{\alpha^{A\varsigma\tau\tau\,2}_{\beta\delta\lambda\,\mu}+\gamma^{A\varsigma\tau\tau\,2}_{\beta\delta\lambda\mu}D^2}{\alpha^{A\varsigma\tau\tau\,2}_{\beta\delta\lambda\mu}+D^2}\right)$$
$$A^{mf}_{\beta\delta\lambda\mu}(\mathbf{D})=A^{0\,mf}_{\beta\delta\lambda\mu}+\frac{1}{2}\left(\frac{\gamma^{A\varsigma\,mf\,1}_{\beta\delta\lambda\mu}D^1}{\alpha^{A\varsigma\,mf\,1}_{\beta\delta\lambda\mu}+D^1}+\frac{\gamma^{A\varsigma\,mf\,2}_{\beta\delta\lambda\mu}D^2}{\alpha^{A\varsigma\,mf\,2}_{\beta\delta\lambda\mu}+D^2}\right) \quad (4.4\text{-}2)$$

where the superscripts $\tau\tau$ stand for membrane gold bending (mm however ff), the superscript ς stands for tension gold compression puts and tensorial subscripts β , δ , λ , μ stand for directions in the plane punt tangent. Discrimination between “tension” gold “compression” status in membrane loading is decided either from the sign of $x=E_{\beta\delta}+\mathbf{Q}^{m\zeta}_{\beta\delta}(\mathbf{D}).\mathbf{E}^{\eta\zeta}$ yew $\beta\delta=\lambda\mu$ however the sign of $x=\mathrm{tr}\left(\mathbf{E}+\mathbf{Q}^{m\zeta}(\mathbf{D}).\mathbf{E}^{\eta\zeta}\right)$, where $\mathbf{Q}^{m\zeta}(\mathbf{D})$ is defined by (3.2-10), and respectively with $\mathbf{K}$ tensor; nevertheless, we decided that the $A^{mf}_{\beta\delta\lambda\mu}$ components doesn' T include this discrimination. This choice allows avoiding any discontinuity of macroscopic resulting stress (3.2-11 and -12), ensuring the convexity of the strain energy density function, according to the general result shown by (Curnier, He, & Zysset, 1995). The $A^{0\tau\tau}_{\beta\delta\lambda\mu}$ and $A^{0\,mf}_{\beta\delta\lambda\mu}$ components corresponds to the sound concrete homogenised elasticity. $A^{0\,mf}_{\beta\delta\lambda\mu}$ is expected to vanish in the box of mirror symmetry, ace said before. That is why we decided to adopt the particular dependency one D^ζ for the $A^{mf}_{\beta\delta\lambda\mu}$ terms, see equation (4.4-2).

Remark 15:

Special This choice of x variable ace status allows custom to uses the direct component of the strain tensor for diagonal terms and year off-diagonal invariant for ones, conserving then the symmetry of tensor $\mathbf{A}$. The compressive function distinguishing tensile but status being not defined when $\mathbf{E}+\mathbf{Q}^{m\zeta}(\mathbf{D})=\mathbf{0}$ (resp. $\mathbf{K}+\mathbf{Q}^{f\zeta}(\mathbf{D})=\mathbf{0}$), arbitrarily, “tension” parameters are affected to the zero macroscopic strain box.

Therefore, there has total of $21\times(1+2\times4)=189$ necessary parameters $A^0_{\beta\delta\lambda\mu}$, α^A and γ^A to fully given the elastic stiffness tensor $\mathbf{A}$, comprising its dissymmetric dependency one macroscopic ramming variables D^1 and D^2 and one tensile but compressive status. Using the Voigt' S notation for matrices, $\mathbf{A}^0$ reads:

$$\begin{pmatrix} A^{0\mathrm{mm}}_{xxxx} & A^{0\mathrm{mm}}_{xxyy} & A^{0\mathrm{mm}}_{xxxy} & A^{0\mathrm{mf}}_{xxxx} & A^{0\mathrm{mf}}_{xxyy} & A^{0\mathrm{mf}}_{xxxy} \\ & A^{0\mathrm{mm}}_{yyyy} & A^{0\mathrm{mm}}_{yyxy} & A^{0\mathrm{mf}}_{yyxx} & A^{0\mathrm{mf}}_{yyyy} & A^{0\mathrm{mf}}_{yyxy} \\ & & A^{0\mathrm{mm}}_{xyxy} & A^{0\mathrm{mf}}_{xyxx} & A^{0\mathrm{mf}}_{xyyy} & A^{0\mathrm{mf}}_{xyxy} \\ & & & A^{0\mathrm{ff}}_{xxxx} & A^{0\mathrm{ff}}_{xxyy} & A^{0\mathrm{ff}}_{xxxy} \\ & & & & A^{0\mathrm{ff}}_{yyyy} & A^{0\mathrm{ff}}_{yyxy} \\ & & & & & A^{0\mathrm{ff}}_{xyxy} \end{pmatrix} \quad (4.4\text{-}3)$$

In order to make easier the comparison with the GLRC_DM constitutive model [R7.01.32], we given edge is equivalent membrane and bending Young' S moduli, and equivalent Poisson' S ratios:

$$E^{mx}_{eq}=\frac{1}{H}\frac{A^{0\mathrm{mm}}_{xxxx}A^{0\mathrm{mm}}_{yyyy}-(A^{0\mathrm{mm}}_{xyxy})^2}{A^{0\mathrm{mm}}_{yyyy}} \quad ; \quad E^{fx}_{eq}=\frac{12}{H^3}\frac{A^{0\mathrm{ff}}_{xxxx}A^{0\mathrm{ff}}_{yyyy}-(A^{0\mathrm{ff}}_{xyxy})^2}{A^{0\mathrm{ff}}_{yyyy}} \quad ; \quad \nu^x_m=\frac{A^{0\mathrm{mm}}_{xxyy}}{A^{0\mathrm{mm}}_{xxxx}} \quad ; \quad \nu^x_f=\frac{A^{0\mathrm{ff}}_{xxyy}}{A^{0\mathrm{ff}}_{xxxx}}$$

where H is the RC punt thickness.

4.4.2 Tensor B

Tensor $\mathbf{B}$ is the coupling elastic ramming-sliding tensor, see equations (3.2-7, - 8). It has symmetric third order tensor of the tangent planes, comprising membrane and bending terms. Possible It is to blind its components using Voigt' S notation: $\mathbf{B}=\begin{pmatrix}\mathbf{B}^{m\zeta}\\ \mathbf{B}^{f\zeta}\end{pmatrix}$, where superscript ζ stands for sliding in the upper ($\zeta=1$) however lower ($\zeta=2$) grid.

Remark 16:

While elastic membrane, and bending corrector fields cuts been computed for both tensile and compressive macroscopic loading, elastic corrector fields $\boldsymbol{\chi}^{\eta^\zeta}$ are obtained for sliding displacement with zero membrane and bending macroscopic loading. Hence tensor $\mathbf{B}$ should include has tension-compression dissymmetry. However, this could introduce has discontinuity in the expression of generalised stress ace soon ace macroscopic sliding strain becomes non-zero, see equations (3.2-11, - 12, - 15). Therefore, we decided to introduce No tension-compression dissymmetry in tensor $\mathbf{B}$.

Hyp. 20. Parameters α^B and γ^B characterising the dependency one the macroscopic ramming D^ζ (Hyp 12) without tensile/compressive distinction are defined. According to Remark 6 see also 8.3, when materials are symmetric relative to the plane Γ_s normal to the sliding bar At not O (i.e tensor $\mathbf{B}$ components vanish. Ace has consequence, there is given No need to “elastic” properties for this tensor. Thus we state:

$$B^{\tau\zeta}_{\beta\delta\lambda}(\mathbf{D})=\frac{\gamma^{B\,\tau\zeta\,1}_{\beta\delta\lambda}D^1}{\alpha^{B\,\tau\zeta\,1}_{\beta\delta\lambda}+D^1}+\frac{\gamma^{B\,\tau\zeta 2}_{\beta\delta\lambda}D^2}{\alpha^{B\,\tau\zeta\,2}_{\beta\delta\lambda}+D^2} \qquad (4.4\text{-}4)$$

where the superscript τ stands for membrane gold bending (m however f), the superscript ζ stands for the zone where sliding takes place (upper gold lower), tensorial subscripts β , δ stand for membrane tangent gold bending directions in the punt planes while tensorial subscript λ stands for sliding strain $E^{\eta\zeta}_\lambda$. There is, with has fixed sliding zone, 6 components for tensors $\mathbf{B}^{m\zeta}$ and $\mathbf{B}^{f\zeta}$ so 24 components for the whole tensor $\mathbf{B}$. Therefore, there has total of $24\times(2\times2)=96$ necessary α^B and γ^B parameters to fully given the coupling elastic ramming-sliding tensor $\mathbf{B}$.

4.4.3 Tensor C

Tensor $\mathbf{C}$ is the sliding elastic “stiffness” tensor, computed from the oven $\boldsymbol{\chi}^{(\eta^\rho_\alpha)}$ sliding auxiliary fields, see equation (3.2-9). It has tangent second order symmetric tensor of the planes of the punt: $C^{\rho\zeta}_{\lambda\mu}=C^{\rho\zeta}_{\mu\lambda}$ (Remark 3). Possible It is to blind $\mathbf{C}$ components using Voigt' S notation. The number of components of tensor $\mathbf{C}$ is then 10 : sliding along x_1 : C^{11}_{11} , C^{22}_{11} , C^{12}_{11} , sliding along x_2 : C^{11}_{22} , C^{22}_{22} , C^{12}_{22} , off-diagonal terms: C^{11}_{12} , C^{22}_{12} , C^{12}_{12} , C^{21}_{12} .

Remark 17:

Ace elastic $\boldsymbol{\chi}^{\eta^\zeta}$ corrector fields are obtained for sliding displacements with zero membrane and bending macroscopic loading, the tensor $\mathbf{C}$ does not include any tension-compression dissymmetry.

Hyp. 21. We define the parameters α^C and γ^C characterising the dependency one macroscopic ramming D^ζ (Hyp 12) of the tensor $\mathbf{C}$ components, without tensile/compressive distinction, by:

$$C_{\lambda\mu}^{\rho\zeta}(\mathbf{D})=\frac{1}{2}C_{\lambda\mu}^{0\rho\zeta}\left(\frac{\alpha_{\lambda\mu}^{C\zeta 1}+\gamma_{\lambda\mu}^{C\zeta 1}D^{1}}{\alpha_{\lambda\mu}^{C\zeta 1}+D^{1}}+\frac{\alpha_{\lambda\mu}^{C\zeta 2}+\gamma_{\lambda\mu}^{C\zeta 2}D^{2}}{\alpha_{\lambda\mu}^{C\zeta 2}+D^{2}}\right) \tag{4.4-5}$$

where the superscripts ρ , ζ stand for the zones where sliding take place (upper gold lower grid), tensorial subscripts λ , μ stands for sliding strain $E_{\lambda}^{\eta\rho}$ and $E_{\mu}^{\eta\zeta}$ directions in the plane punt tangent. Therefore, accounting for the symmetry of this tensor, there has total of $10\times(1+2\times 2)=50$ necessary $C_{\lambda\mu}^{0\rho\zeta}$, α^{C} and γ^{C} parameters to fully given the sliding elastic “stiffness” tensor $\mathbf{C}$. Using the Voigt' S notation for matrices, $\mathbf{C}^{0}$ reads:

$$\begin{pmatrix} C_{xx}^{011} & C_{yx}^{011} & C_{xx}^{012} & C_{yx}^{012} \\ & C_{yy}^{011} & C_{xy}^{012} & C_{yy}^{012} \\ & & C_{xx}^{022} & C_{yx}^{012} \\ & & & C_{yy}^{022} \end{pmatrix} \tag{4.4-6}$$

To sum up, we need to identify 335 parameters after linear FEM RVE calculations:

- 21 upper diagonal terms $A_{\beta\delta\lambda\mu}^{0}$ for the fourth order symmetric sound elastic punt tensor (membrane more bending);
- 42 terms $\alpha_{\beta\delta\lambda\mu}^{A\varsigma\tau\zeta}$ and 42 terms $\gamma_{\beta\delta\lambda\mu}^{A\varsigma\tau\zeta}$ in the traction domain and the same number for the compression domain, describing the dependency of tensor A one ramming D^{ζ} ;
- 48 terms $\alpha_{\beta\delta\lambda}^{B\varsigma\zeta}$ and 48 terms $\gamma_{\beta\delta\lambda}^{B\varsigma\zeta}$ describing the dependency of tensor $\mathbf{B}$ one ramming D^{ζ} ;
- 10 upper diagonal terms $C_{\beta\delta}^{0\zeta}$ for the second order symmetric sliding tensor;
- 20 terms $\alpha_{\beta\delta}^{C\zeta\rho}$ and 20 terms $\gamma_{\beta\delta}^{C\zeta\rho}$ describing the dependency of tensor $\mathbf{C}$ one ramming D^{ζ} .

Remark 18:

In practice, due to the isotropy of undamaged concrete and the symmetry in plane (x_1, x_2) of the steel rebar in the RVE, this amount of parameters edge Be reduced to 249 . Indeed, in that box eight components $\langle\langle a_{\alpha\beta\gamma\delta}^{k}(d)\rangle\rangle_{\Omega}$ vanish, since $a_{1112}^{k}=0$ and so one, and we edge prove from auxiliary problems (3.1-5) that the corresponding cross-country race-product averages (e.g. $\langle\langle \varepsilon_{ij}(\boldsymbol{\chi}^{11}):a_{ijkl}^{k}(d):\varepsilon_{kl}(\boldsymbol{\chi}^{12})\rangle\rangle_{\Omega}$) vanish too. So, eight of $A_{\beta\delta\lambda\mu}^{0}$ components vanish (e.g. A_{1112}^{0}). Ace far ace that goes, eight of γ^{B} parameters (e.g. γ_{121}^{Bm11}), six components of $C_{\beta\delta}^{0\rho\zeta}$ vanish, so this last tensor becomes diagonal.

4.4.4 Jump-sliding limit

The last physical parameter to define more precisely is the jump-sliding limit σ_{crit}^{ζ} . Indeed experimental year been worth τ_{crit} is provided by usual sweater-out tests, where has rebar centred in has concrete hexaedral volume is tensioned until sliding. According to Hyp.3 and Hyp.11., this been worth – assumed to Be identical whatever the rebar – has to Be adapted to the particular situation of the jump-sliding process in the RC RVE, for authority for has given pure links tensile uniaxial membrane resulting stress $N_{\alpha\alpha}^{t}$, in the x_{α} direction. Ace sliding edge occur only yew ramming is non-uniform within the RVE, see Hyp.7 and section 8.3, we adopt

has RVE Ω_α , with has prescribed d^ζ been worth in concrete sub-domain Ω_{dm}^ζ . From auxiliary field solutions in membrane $\boldsymbol{\chi}^{\alpha\beta}$ and bending $\boldsymbol{\xi}^{\alpha\beta}$ combined for the macroscopic strain measures $\mathbf{A}^{-1}(D^\zeta).N_{\alpha\alpha}^t$, with zero sliding ($\mathbf{E}^{\eta\zeta}=\mathbf{0}$, we given edge easily the steel resulting stress $F_{N_{\alpha\alpha}^t}^\zeta$ in the central section (At cutting Γ_s interface) of the considered bar $\Omega_s^{x_\alpha\,\zeta}$ in the x_α direction. Resulting Therefore, the $F_{N_{\alpha\alpha}^t}^\zeta$ has linear combination obtained from the corresponding links contribution of each auxiliary field $\boldsymbol{\chi}^{\alpha\beta}$ in membrane, and $\boldsymbol{\xi}^{\alpha\beta}$ in bending, for the selected non-zero been worth of d^ζ , one RVE Ω_X and Ω_Y . Ace far ace that goes, we calculate the corresponding $\boldsymbol{\Sigma}_{\alpha\,N_{\alpha\alpha}^t}^{\eta\zeta}$ sliding stress, applying (3.2-15). From (3.2-23), equating with $\Sigma_\alpha^{\zeta\,crit}$ been worth defined by the σ_{crit}^ζ debonding been worth, we given the critical been worth $\tilde{N}_{\alpha\alpha}^t$, thus the corresponding been worth of steel resulting stress $\tilde{F}_{N_{\alpha\alpha}^t}^\zeta$ which has to Be equal to $\tau_{crit}\left|\Gamma_b^\zeta\right|/2$. Therefore, we get the jump-sliding threshold constant:

$$\sigma_{crit}^\zeta=\tau_{crit}\frac{|\Omega|}{H}\frac{|\boldsymbol{\Sigma}_{\alpha\,N_{\alpha\alpha}^t}^{\eta\zeta}|}{|F_{N_{\alpha\alpha}^t}^\zeta|}\qquad\Rightarrow\quad\Sigma_\alpha^{\zeta\,crit}=\frac{H\left|\Gamma_b^\zeta\right|}{2|\Omega|}\sigma_{crit}^\zeta=\frac{\left|\Gamma_b^\zeta\right|}{2}.\frac{|\boldsymbol{\Sigma}_{\alpha\,N_{\alpha\alpha}^t}^{\eta\zeta}|}{|F_{N_{\alpha\,\alpha}^t}^\zeta|}\tau_{crit}\tag{4.4-7}$$

4.5 Automated procedure

The 342 linear elastic auxiliary problems edge Be easily solved by finite elements, using only 11 geometrical parameters and 10 material parameters to define the whole RVE mechanical model. Thesis parameters are in practice the ones required from practitioners to identify DHRC parameters set.

In order to make easy the parameter identification, year automated procedure has been implemented in *Salomé-Méca*. The approximate CPU time needed is about 5 minutes one has usual personal computer.

Steel rebar are represented by cylinders of hand axis x_1 however x_2 . Year example of has mesh for the numerical links concealment is presented one Figure 4 1. This example concerns young stag has punt of $20\,cm$ of thickness with has steel proportion of $0.8\,\%$ and has steel rebar spacing of $12{,}5\,cm$.

Remark 19:

Steel rebar oriented in the x_1 however x_2 directions of has same steel grid figures has different position in the thickness of the punt (i.e along the x_3 direction), then inducing has significant variation in the bending stiffness of the punt around x_1 however x_2 .

For all the simulations presented young stag, the links concealment mesh is composed of linear tetrahedral finite elements refined in the vicinity of steel rebar in order to re-press possible ace much ace to their cylindrical geometry. The average number of dismantle of freedom considered is of $100\,000$.

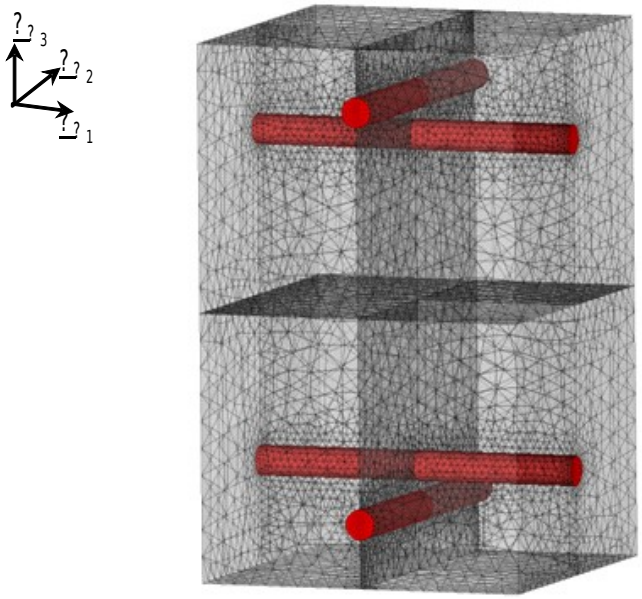

Figure 4 1. Example of has links RVE mesh for parameters identification (red: steel rebar, grey: concrete).

Year automated *python*™ process generates automatically the RVE mesh from the following eleven geometrical parameters:

1.	Punt thickness	H
2. and 3.	Steel rebar spacing along x_1 and x_2	ex and ey
4. 5. 6. and 7.	Diameters of the oven steel rebar	
8. 9. 10. and 11.	x_3 positions of the oven steel rebar	

Steel-concrete This three-dimensional mesh includes the splitting of nodes located one interfaces (surfaces Γ_b^ζ), the assignment of the different mesh zones to the sub-domains Ω_i^1 , Ω_i^2 , and periodicity of node hirings for the external boundaries (normal links vectors along x_1 and x_2). Microscopic material properties and boundary conditions prescribing, including periodicity in the RVE outer surfaces (upper and lower surfaces remaining free) and jump slipway basis function are set.

Concerning the ten needed material parameters, the following table gathers the expected been worth:

2 elastic coefficients for steel	Young' S modulus, Poisson' S ratio	E_s , ν_s
2 elastic coefficients for concrete	Young' S modulus, Poisson' S ratio	E_c , ν_c
Concrete Usual engineering parameters for	Tensile and compressive strengths, maximum compressive strain, first compressive ramming limit	f_t , f_c , ε_{cm} , f_{dc}
	Steel-concrete sweater-out sliding experimental threshold parameter	τ_{crit}

	Tensile Post-peak path parameter of local concrete constitutive relation	γ_+

They are required in order to perform the 342 FEM elastic calculations one the RVE, see the table reported in the Appendix, At section 7.1, and DHRC threshold parameters determination.

The results of the numerical finite element simulations are used to identify the 335 DHRC macroscopic parameters with the help of has standard least public garden algorithm.

Remark 20:

In practice, yew the obtained been worth of macroscopic coefficients of $\mathbf{A}^{mf}(\mathbf{D})$ *,* $\mathbf{C}(\mathbf{D})$ *matrices are very small, and making consequently impossible the parameter identification, we decide to take the corresponding* α *,* γ^A *,* γ^C *parameters equal to* 1 *and* γ^B *parameters equal to* 0 *.*

4.6 Commonplace Analytical example

To illustrate the implementation of the previous approach, we take the following representative analytical commonplace example.

The first step consists in verifying that the automatic procedure recovers the usual isotropic linear elastic punt stiffness tensor yew we take, in the whole RVE, the same uniform sound elastic characteristics (E , ν). Indeed, in that box, the RVE Ω is reduced to the simple segment $]-H/2,H/2[$ along the axis $(O\mathbf{e}_{(x_3)})$), and all the auxiliary fields $\boldsymbol{\chi}^{\alpha\beta}$ in membrane and $\boldsymbol{\xi}^{\alpha\beta}$ in bending only one depends x_3 . Solving in such situation the auxiliary problems (3-4), using first trial $\mathbf{v}(x_3)$ functions $(v_{1,}v_{2,}0)$ then $(0,0,v_3)$, we obtain easily:

$$\boldsymbol{\chi}^{\alpha\alpha}=-\frac{\nu}{1-\nu}(0,0,x_3) \quad ; \quad \boldsymbol{\chi}^{12}=(0,0,0) \quad ; \quad \boldsymbol{\xi}^{\alpha\alpha}=-\frac{\nu}{2(1-\nu)}(0,0,x_3^2) \quad ; \quad \boldsymbol{\xi}^{12}=(0,0,0) \tag{4.6-1}$$

Hence the macroscopic homogenised elastic punt tensor $\mathbf{A}$ are:

$$\begin{gathered} A^{mm}_{\alpha\alpha\alpha\alpha}=EH/(1-\nu^2) \quad ; \quad A^{mm}_{\alpha\alpha\beta\beta}=\nu EH/(1-\nu^2) \quad ; \quad A^{mm}_{1212}=EH/2(1+\nu) \quad ; \\ A^{ff}_{\alpha\alpha\alpha\alpha}=(EH^3)/12(1-\nu^2) \quad ; \quad A^{ff}_{\alpha\alpha\beta\beta}=(\nu EH^3)/12(1-\nu^2) \quad ; \quad A^{ff}_{1212}=(EH^3)/24(1+\nu) \\ ; \quad \mathbf{A}^{mf}=\mathbf{0} \end{gathered} \tag{4.6-2}$$

4.7 Constitutive Comparison of parameters with other models

In order to give to use comparative information about DHRC parameters, with respect to other constitutive models, like GLRC_DM [R7.01.32], we proposes the following evaluation in monoaxial loading boxes, first in membrane, then in bending. The information are calculated by the DHRC

constitutive model automated identification procedure. So it is more easy to observes the influence of RVE material dated one the DHRC parameters, before to perform the structural analysis itself.

4.7.1 Elastic coefficients

We refer to the GLRC_DM model [R7.01.32], § 3.1, to fast the RC are equivalent elastic moduli in membrane (E_{eq}^{m}) and in bending (E_{eq}^{f}), from material dated (concrete E_b , ν_b and steel E_a moduli) and geometrical dated (steel section S_a , thickness h , relative position of steel rebar in the thickness $\chi_a \in]0,1[$):

$$\begin{aligned} E_{eq}^{m} &= E_a \frac{S_a}{h} + E_b \cdot \frac{E_b h + E_a S_a}{E_b h + E_a S_a (1-\nu_b^2)} \quad ; \\ E_{eq}^{f} &= \frac{3}{h} E_a S_a \chi_a^2 + E_b \cdot \frac{E_b h + 3 E_a S_a \chi_a^2}{E_b h + 3 E_a S_a \chi_a^2 (1-\nu_b^2)} \end{aligned} \tag{4.7-1}$$

Therefore, the equivalent elastic RC punt coefficients in uniaxial membrane and in uniaxial bending edge Be deduced by:

$$A_{eq_{GLRC}}^{0\,mm} = E_{eq}^{m} h \quad ; \quad A_{eq_{GLRC}}^{0\,ff} = E_{eq}^{f} \frac{h^3}{12} \tag{4.7-2}$$

According to the DHRC formulation in elastic domain, particular tensor $\mathbf{A}^0$, we fast edge the membrane resulting stress in uniaxial loading box in terms of membrane uniaxial strain, both x and y steel grids directions, and in the same way for the uniaxial bending box; we get then:

$$\begin{pmatrix} \varepsilon_{xx} \\ \varepsilon_{yy} \\ \gamma_{xy} \\ \kappa_{xx} \\ \kappa_{yy} \\ \kappa_{xy} \end{pmatrix} = \left(\mathbf{A}^0\right)^{-1} \cdot \begin{pmatrix} N_{xx} \\ 0 \\ 0 \\ 0 \\ 0 \\ 0 \end{pmatrix} \quad ; \quad \begin{pmatrix} \varepsilon_{xx} \\ \varepsilon_{yy} \\ \gamma_{xy} \\ \kappa_{xx} \\ \kappa_{yy} \\ \kappa_{xy} \end{pmatrix} = \left(\mathbf{A}^0\right)^{-1} \cdot \begin{pmatrix} 0 \\ 0 \\ 0 \\ M_{xx} \\ 0 \\ 0 \end{pmatrix} \tag{4.7-3}$$

After elimination of all generalised strain variable except respectively ϵ_{xx} however κ_{xx} , we easily derived the expressions of the equivalent elastic RC punt coefficients in uniaxial membrane and in uniaxial bending for the DHRC constitutive model, in the x steel grid direction, to Be compared with the closed forms GLRC_DM model ones:

$$A_{eq_{DHRC}}^{0\,mm} = \left(\left(\mathbf{A}^0\right)^{-1}_{\epsilon_{xx}} \right)^{-1} \quad ; \quad A_{eq_{DHRC}}^{0\,ff} = \left(\left(\mathbf{A}^0\right)^{-1}_{\kappa_{xx}} \right)^{-1} \tag{4.7-4}$$

To Be more specifies, the same calculations are also performed with the only mixture law contributions to tensor $\mathbf{A}^0$, see section 3.2: this allows to observes the influence of auxiliary fields one final results.

We out curry the same calculations for the y steel grid direction.

4.7.2 Post-elastic coefficients

In order to check the post-elastic answer of the DHRC constitutive model, we calculable At the state $\mathbf{D}=\mathbf{0}$ and $\dot{\mathbf{D}}>\mathbf{0}$ the disastrous of resulting stresses in radial monoaxial loading paths in disastrous respect of of the generalised strain variable, provided we cuts distinguished compressive then tensile boxes for membrane loading. According to relations (3.2-11) and (3.2.12):

$$\begin{pmatrix}\dot{\mathbf{N}}\\ \dot{\mathbf{M}}\end{pmatrix}=\begin{bmatrix}\mathbf{A}^{0\,mm} & \mathbf{A}^{0\,mf}\\ \mathbf{A}^{0\,fm} & \mathbf{A}^{0\,ff}\end{bmatrix}:\begin{pmatrix}\dot{\mathbf{E}}\\ \dot{\mathbf{K}}\end{pmatrix}+\dot{\mathbf{D}}.\begin{bmatrix}\mathbf{A}^{mm}_{,\mathbf{D}}(\mathbf{0}) & \mathbf{A}^{mf}_{,\mathbf{D}}(\mathbf{0})\\ \mathbf{A}^{fm}_{,\mathbf{D}}(\mathbf{0}) & \mathbf{A}^{ff}_{,\mathbf{D}}(\mathbf{0})\end{bmatrix}:\begin{pmatrix}\mathbf{E}\\ \mathbf{K}\end{pmatrix} \tag{4.7-5}$$

According to (4.4-2), we recall that derivative $\mathbf{A}_{,\mathbf{D}}(\mathbf{0})$ are directly depend one tensor $\mathbf{A}^0$ and α^A and γ^A parameters, respectively in has tensile, compressive membrane, but positive but negative bending state. Moreover, the consistency conditions $\dot{f}_{(d^p)}=0$ give:

$$\dot{\mathbf{D}}=\frac{-2\begin{pmatrix}\mathbf{E}\\ \mathbf{K}\end{pmatrix}:\begin{bmatrix}\mathbf{A}^{mm}_{,\mathbf{D}}(\mathbf{0}) & \mathbf{A}^{mf}_{,\mathbf{D}}(\mathbf{0})\\ \mathbf{A}^{fm}_{,\mathbf{D}}(\mathbf{0}) & \mathbf{A}^{ff}_{,\mathbf{D}}(\mathbf{0})\end{bmatrix}:\begin{pmatrix}\dot{\mathbf{E}}\\ \dot{\mathbf{K}}\end{pmatrix}}{\begin{pmatrix}\mathbf{E}\\ \mathbf{K}\end{pmatrix}:\begin{bmatrix}\mathbf{A}^{mm}_{,\mathbf{DD}}(\mathbf{0}) & \mathbf{A}^{mf}_{,\mathbf{DD}}(\mathbf{0})\\ \mathbf{A}^{fm}_{,\mathbf{DD}}(\mathbf{0}) & \mathbf{A}^{ff}_{,\mathbf{DD}}(\mathbf{0})\end{bmatrix}:\begin{pmatrix}\mathbf{E}\\ \mathbf{K}\end{pmatrix}} \tag{4.7-6}$$

Radial ace we consider loading paths controlled by has regular $h(t)$ function, we edge Write:

$$\begin{pmatrix}\dot{\mathbf{E}}\\ \dot{\mathbf{K}}\end{pmatrix}=\dot{h}(t).\begin{pmatrix}\mathbf{E}_1\\ \mathbf{K}_1\end{pmatrix} \tag{4.7-7}$$

So we edge disastrous Write the equations in has concise manner:

$$\begin{pmatrix}\dot{\mathbf{N}}\\ \dot{\mathbf{M}}\end{pmatrix}=\begin{bmatrix}\mathbf{A}^{T\,mm} & \mathbf{A}^{T\,mf}\\ \mathbf{A}^{T\,fm} & \mathbf{A}^{T\,ff}\end{bmatrix}:\begin{pmatrix}\dot{\mathbf{E}}\\ \dot{\mathbf{K}}\end{pmatrix} \tag{4.7-8}$$

where tensor $\mathbf{A}^T$ results from contribution of $\mathbf{A}^0$ and to their derivative At $\mathbf{D}=\mathbf{0}$, see equations (4.7-5) and (4.7-6) applied for the directions $(\mathbf{E}_1\ ,\ \mathbf{K}_1)$. And we apply to tensor $\mathbf{A}^T$ the same procedure than gives for tensor $\mathbf{A}^0$ At section 4.7.1 to calculate the equivalent post-elastic RC punt disastrous coefficients in uniaxial membrane (compressive then tensile boxes) and in uniaxial bending for the DHRC constitutive model, in the x steel grid direction, then in y steel grid direction.

We refer to the GLRC_DM model [R7.01.32], § 3.2.2.1 and § 3.2.2.3, to fast the RC are equivalent post-elastic disastrous coefficients in membrane and in bending, I order to make comparison with DHRC constitutive model. We edge also prefer to make this comparison with asymptotic slopes of membrane and bending answers of GLRC_DM model, see [R7.01.32], § 3.2.3.1 and § 3.2.3.3. Nevertheless, we edge adopt the simplified expressions given in [R7.01.32], § 3.2.4.1 and § 3.2.4.3, involving γ_{mt}, γ_{mc}, γ_f GLRC_DM parameters, acting ace proportional reduction factors one elastic coefficients.

4.8 Internal variables of the DHRC model

The internal variable output of *Code_Aster* are the following: the six fist are true thermodynamic internal variable, the five last ones are produced for easier post-treatment.

variables	name	content
V1	'ENDOSUP'	D_1 Ramming in the upper half of RVE
V2	'ENDOINF'	D_2 Ramming in the lower half of RVE
V3	'GLISXSUP'	$E_x^{\eta 1}$ jump sliding of x rebar in the upper half of RVE
V4	'GLISYSUP'	$E_y^{\eta 1}$ jump sliding of y rebar in the upper half of RVE
V5	'GLISXINF'	$E_x^{\eta 2}$ jump sliding of x rebar in the lower half of RVE
V6	'GLISYINF'	$E_y^{\eta 2}$ jump sliding of y rebar in the lower half of RVE
V7	'DISSENDO'	Dissipated energy by ramming: $D_{diss}^{endo}(t)=G_1^{crit} D_1(t)+G_2^{crit} D_2(t)$
V8	'DISSGLIS'	Dissipated energy by jump sliding: $D_{diss}^{bond-slide}(t)= \Sigma_x^{crit\,1}\int_0^t \dot{E}_x^{\eta 1} dt+\Sigma_y^{crit\,1}\int_0^t \dot{E}_y^{\eta 1} dt+\Sigma_x^{crit\,2}\int_0^t \dot{E}_x^{\eta 2} dt+\Sigma_y^{crit\,2}\int_0^t \dot{E}_y^{\eta 2} dt$
V9	'DISSIP'	Sum of both energy dissipations
V10	'ADOUMEMB'	Mean relative weakening of concrete membrane stiffness of reinforced slab
V11	'ADOUFLEX'	Mean relative weakening of bending stiffness of reinforced concrete slab

Distinction between upper and lower faces is made from the orientation of the local reference frame At each Gauss' not. So, the lower face is damaged $\dot{D}_2>0$ for positive punt increasing curvatures, whereas the upper one is damaged $\dot{D}_1>0$ for negative curvatures.

The $V10$ and $V11$ been worth comparable are to the scalar equivalent variable being produced by the GLRC_DM model, see [R7.01.32], to describe roughly the stiffness degradation of the RC punt. Respective The calculated expressions are At each time-step:

$$V10=1-\sqrt[3]{A_{xxxx}^{mm}(\mathbf{D})\,A_{yyyy}^{mm}(\mathbf{D})\,A_{xxyy}^{mm}(\mathbf{D})}/\sqrt[3]{A_{xxxx}^{0\mathrm{mm}}\,A_{yyyy}^{0\mathrm{mm}}\,A_{xxyy}^{0\mathrm{mm}}}$$
$$V11=1-\sqrt[3]{A_{xxxx}^{ff}(\mathbf{D})\,A_{yyyy}^{ff}(\mathbf{D})\,A_{xxyy}^{ff}(\mathbf{D})}/\sqrt[3]{A_{xxxx}^{0\mathrm{ff}}\,A_{yyyy}^{0\mathrm{ff}}\,A_{xxyy}^{0\mathrm{ff}}} \quad (4.8\text{-}1)$$

They are being zero in absence of ramming. Thesis two variable neglect membrane-bending coupling.

5 Verification

The model is verified by means of the test-boxes: SSNS106C, H, I, J, L, M, NR, O see [bib8], comparing with the GLRC_DM model results, whose parameters are identified in has consist way and the ENDO_ISOT_BETON constitutive concrete relation for and elastic rebar grids in has multi-to bush-hammer RC punt modelling. The studied boxes are:

ssns106 C	Tensile-compressive with bending coupling loading cycle, low load level
ssns106 H	Tensile-compressive loading cycle, high load level
ssns106 I	Pure bending alternate cyclic loading, high load level
ssns106 J	Tensile-compressive with bending coupling loading cycle, high load level
ssns106 L	Pure shear stress and shear strain alternate cyclic in plane loading, high load level
snss106 m	Pure shear stress and bending coupling alternate cyclic in plane loading, high load level
ssns106 N	Anticlastic bending alternate cyclic in plane loading, high load level
ssns106 O	Pure Thermoelastic membrane loading cycle

Post-elastic shear answers of the two DHRC and GLRC_DM models different are significantly. Indeed, the calibration gives to align the two models in tension is No to skirt effective in shear strain stemming from the fact that DHRC shear strain behavior comes from the identification of the parameters by homogenization while with the GLRC_DM model this behavior is deduced from tensile and compressive answers working in the eigen-frame of the macroscopic membrane strains. Furthermore, the primary ramming thresholds been worth GLRC_DM and DHRC are has little different bit. We edge observes the significant contribution of sliding in the total dissipated energy obtained by the DHRC constitutive model, which is not get-At-whitebait by the GLRC_DM one. Moreover, we observes that with model we get year increasing ramming At each alternate cycle, which is not reproduced with the GLRC_DM one.

6 Validation

The model is validated by means of comparison one summons experimental dated one reinforced concrete structures. The first one is year alternate compressive-tensile test one has reinforced concrete member, see test-boxes: SSNS112 , [bib18]. The second one considers has reinforced concrete beam under monotonic bending, see test-boxes: SSNL119 , [bib19]. The third one considers has reinforced concrete shear wall, under alternate increasing shear loading cycles, see test-boxes: SSNS113 , [bib20].

7 References

Note: the references to published materials quoted in the previous sections are available in [feeding-bottle 13].

1. LEMAITRE J., CHABOCHE J.L.: “Mechanical of solid materials”, ED. Dunod (1985)

2. P.KOECHLIN, S.POTAPOV. “With total constitutive model for reinforced concrete punts”. ASCE J. Eng. Mech. 2006.

3. P.KOECHLIN, S.MILL. “Model of total behavior of the reinforced concrete plates under dynamic loading in inflection: improved law GLRC: modeling of cracking by damage”. Note HT-62/02/021/A, 11/2002.

4. F.VOLDOIRE. “Homogenisation of the heterogeneous structures”. Note EDF/DER/MMN HI-74/93/055, 10/27/1993.

5. S.MILL. “Modeling of the reinforced concrete structures under seismic loading”. Note HT-62/04/025/A, 12/2004.

6. S.MILL. F.VOLDOIRE “Study of a reinforced concrete beam under loading of inflection”. Note HT-62/05/013/A, 9/2006.

7. J-J.MARIGO. “Digital study of the damage”. EDF, Bulletin of the studies and research, series C, n°2, pp. 27-48, 1982.

8. [V6.05.106] SSNS106 – Degradation of a reinforced concrete plate under requests varied with the total laws GLRC_DM. and DHRC.

9. [R3.07.03] – Elements of plate DKT, DST, DKQ, DSQ and Q4G.

10. [R7.01.04] – Law of behavior ENDO_ISOT_BETON.

11. [R7.01.32] – Law of behavior GLRC_DM .

12. Ch.COMBESCURE; H.DUMONTET, F.VOLDOIRE. Constitutive Homogenised model coupling ramming and debonding for reinforced concrete structures under cyclic requests. Int. J. Ground. Struct., 50, pp. 3861-3874, 2013.

13. Ch.COMBESCURE; H.DUMONTET, F.VOLDOIRE. Dissipative Homogenised Reinforced Concrete (DHRC) constitutive model dedicated to reinforced concrete punts under seismic loading. Int. J. Ground. Struct., to Be published, 2015.

14. Ch.COMBESCURE. Formulation of a homogenized model of reinforced concrete plate for seismic applications. Doctorate of the university Pierre and Marie Curie, constant on September 25th, 2013.

15. P.SUQUET, 1982. Plasticity and homogenisation. Thesis of State, University Paris VI.

16. D.CAILLERIE, 1984. Thin elastic periodic punts. Maths. Methods Appl. Sci. 6,159-191.

17. F.VOLDOIRE, 1993. Homogenisation of the heterogeneous structures, Collar. Notes interns DER, ISSN 1161-059X, 1161-0611, Paris.

18. [V6.05.106] SSNS112 – Test of compression and tensile of a reinforced concrete post.
19. [V6.02.119] SSNL119 – Response static of a reinforced concrete beam (rectangular section) to nonlinear behavior.
20. [V6.05.113] SSNS113 – Simulation of test TESSH.

8 Withppendix

8.1 Auxiliary problems counts

We edge find in the following table the sequence of 342 auxiliary problems calculation management, for membrane, bending and jump-sliding boxes, for the different been worth of ramming variables, used in the automated DHRC parameters identification procedure.

EAR been worth	Been worth PRE_ EPSI	Calculations number		Membrane index		Bending index		Sliding index		RVE	Loading	Ramming	Sliding	Membrane with. field	Bending with. field
-1	1	1	9	0	8	0	8	-	-	1X and 2X	compression X	yes	No	χ_c^{xx}	ξ_c^{xx}
1	-1	10	18	9	17	9	17	-	-	1X and 2X	tension X	yes	No	χ_t^{xx}	ξ_t^{xx}
-1	1	19	27	18	26	18	26	-	-	1X and 2X	compression Y	yes	No	χ_c^{yy}	ξ_c^{yy}
1	-1	28	36	27	35	27	35	-	-	1X and 2X	tension Y	yes	No	χ_t^{yy}	ξ_t^{yy}
0.5	-0.5	37	45	36	44	36	44	-	-	1X and 2X	shear	yes	No	χ^{xy}	ξ^{xy}
-1	1	46	54	45	53	45	53	-	-	1Y and 2Y	compression X	yes	No	χ_c^{xx}	ξ_c^{xx}
1	-1	55	63	54	62	54	62	-	-	1Y and 2Y	tension X	yes	No	χ_t^{xx}	ξ_t^{xx}
-1	1	64	72	63	71	63	71	-	-	1Y and 2Y	compression Y	yes	No	χ_c^{yy}	ξ_c^{yy}
1	-1	73	81	72	80	72	80	-	-	1Y and 2Y	tension Y	yes	No	χ_t^{yy}	ξ_t^{yy}
0.5	-0.5	82	90	81	89	81	89	-	-	1Y and 2Y	shear	yes	No	χ^{xy}	ξ^{xy}
-1	1	91	99	90	98	90	98	-	-	1T and 2T	compression X	yes	No	χ_c^{xx}	ξ_c^{xx}
1	-1	100	108	99	107	99	107	-	-	1T and 2T	tension X	yes	No	χ_t^{xx}	ξ_t^{xx}
-1	1	109	117	108	116	108	116	-	-	1T and 2T	compression Y	yes	No	χ_c^{yy}	ξ_c^{yy}
1	-1	118	126	117	125	117	125	-	-	1T and 2T	tension Y	yes	No	χ_t^{yy}	ξ_t^{yy}
0.5	-0.5	127	135	126	134	126	134	-	-	1T and 2T	shear	yes	No	χ^{xy}	ξ^{xy}
0	0	136	144	135	143	-	-	0	8	1X and 2X	-	No	1X		
0	0	145	153	144	152	-	-	9	17	1X and 2X	-	No	2X		
0	0	154	162	153	161	-	-	18	26	1X and 2X	-	No	1Y		
0	0	163	171	162	170	-	-	27	35	1X and	-	No	2Y		

										2X				
0	0	172	180	171	179	-	-	36	44	1Y and 2Y	-	No	1X	
0	0	181	189	180	188	-	-	45	53	1Y and 2Y	-	No	2X	
0	0	190	198	189	197	-	-	54	62	1Y and 2Y	-	No	1Y	
0	0	199	207	198	206	-	-	63	71	1Y and 2Y	-	No	2Y	

8.2 Convexity of the strain energy density function with discontinuity in ramming function

Ace presented in section 3.1.2, the macroscopic free energy density $W\left(\mathbf{E},\mathbf{K},D^{\zeta},\mathbf{E}^{\eta\zeta}\right)$ is continuous when its variable are taken in the whole strains and sliding strains space. However, the discontinuity in microscopic ramming functions $\xi(d)$ – had to the assumed tensile distinction between and compressive states, see Hyp 14 – induces has part-wise definition of the elasticity tensors $\mathbf{A}^{mm}(\mathbf{D})$ and $\mathbf{A}^{ff}(\mathbf{D})$, while $\mathbf{A}^{mf}(\mathbf{D})$ components don' T include this dissymmetry. We recall that, according to Remark 16, $\mathbf{B}(\mathbf{D})$ and $\mathbf{C}(\mathbf{D})$ tensors don' T entail any tension-compression dissymmetry. In domains sufficiently far from this discontinuity, it edge Be easily shown the convexity of the strain energy density function from its quadratic expression. Conversely, either side of this discontinuity, we cuts to proceed ace proposed for authority by (Curnier, He, & Zysset, 1995).
Ace being assumed At Hyp 19, the discontinuity is defined by the hyperplane $\mathbf{E}+\mathbf{Q}^{m\zeta}(\mathbf{D}).\mathbf{E}^{\eta\zeta}=\mathbf{0}$ and $\mathbf{K}+\mathbf{Q}^{f\zeta}(\mathbf{D}).\mathbf{E}^{\eta\zeta}=\mathbf{0}$, for $\mathbf{D}$ being fixed, with $\mathbf{Q}^{\zeta}(\mathbf{D})=\mathbf{A}^{(-1)}(\mathbf{D}):\mathbf{B}^{\zeta}(\mathbf{D})$ defined by (3.2-10).
We take profit that the resulting stresses (3.2-11 and -12) obtained by derivation of the strain energy density function are continuous by construction with the discontinuity of $\mathbf{A}^{mm}(\mathbf{D})$ and $\mathbf{A}^{ff}(\mathbf{D})$ defined by the sign of x . Nevertheless, aces we need to fast the updated been worth of $\mathbf{A}^{mm}(\mathbf{D})$ and $\mathbf{A}^{ff}(\mathbf{D})$ components to given $\mathbf{Q}^{\zeta}(\mathbf{D})$ At each step increment, we decided to input the previous been worth $\mathbf{D}^{-}$, in year explicit algorithm way, see section 4 .

8.3 Proof of the zero-valued tensor $\mathbf{B}$ yew microscopic ramming field is homogeneous in the RVE

Let custom recall that the tensor $\mathbf{B}$ components are defined by: $B^{m\zeta}_{\alpha\beta\gamma}(\mathbf{D})=\left\langle\left\langle a_{\alpha\beta kl}(d):\varepsilon_{kl}\left(\boldsymbol{\chi}^{\eta_\gamma^\zeta}\right)\right\rangle\right\rangle_{\Omega}$ and $B^{f\zeta}_{\alpha\beta\gamma}(\mathbf{D})=-\left\langle\left\langle x_3.a_{\alpha\beta kl}(d):\varepsilon_{kl}\left(\boldsymbol{\chi}^{\eta_\gamma^\zeta}\right)\right\rangle\right\rangle_{\Omega}$, see (3.2-7 and -8). Let custom assumes that the components of the concrete damaged elastic tensor $a^{c}_{pqrs}\left(d^{\zeta}\right)$ are symmetric with respect to the plane $x_1=0$, i.e. Γ_s see Figure 2.1.4-a; moreover, according to the section 2.1.4, this tensor fulfils the symmetries with respect to the reference frame. Let custom consider the auxiliary problem (3-1.5) concerning the corrector $\boldsymbol{\chi}^{\eta_1^\zeta}$ associated to sliding in the x_1 direction. Necessarily, we cuts the following properties: $\chi_1^{\eta_1^\zeta}$ is symmetric with respect to the plane $x_1=0$, whereas $\chi_2^{\eta_1^\zeta}$ and $\chi_3^{\eta_1^\zeta}$ are antisymmetric. Therefore, $a_{iikl}(d):\varepsilon_{kl}\left(\boldsymbol{\chi}^{\eta_1^\zeta}\right)$ and $a_{23\mathrm{kl}}(d):\varepsilon_{kl}\left(\boldsymbol{\chi}^{\eta_1^\zeta}\right)$ are antisymmetric with respect to the plane $x_1=0$, whereas $a_{1\mathrm{jkl}}(d):\varepsilon_{kl}\left(\boldsymbol{\chi}^{\eta_1^\zeta}\right)$ are symmetric, for $j\neq 1$ and $a_{1\mathrm{jkl}}(d):\varepsilon_{kl}\left(\boldsymbol{\chi}^{\eta_1^\zeta}\right)$ are antisymmetric with respect to the plane $x_2=0$.

Performing the integration one the whole RVE, we deduce that: $B^{m\zeta}_{\alpha\beta 1}(\mathbf{D})$ and $B^{f\,\zeta}_{\alpha\beta 1}(\mathbf{D})$ vanish. The same reasoning holds for the other mid-plane direction in of the RVE.

Since the tensor $\mathbf{B}$ manage the coupling between RC punt kinematics and steel jump sliding, we conclude that jump sliding edge occur only yew symmetry loss appears in the RVE, due to ramming.